Dalton Transactions

PERSPECTIVE

View Article Online
View Journal

Cite this: DOI: 10.1039/d6dt00012f

Purine-derived N-heterocyclic carbene metal complexes: catalytic applications and reactivity

Alejandro Cervantes-Reyes, *[a] Ricardo Malpica-Calderón,[a] Hugo Valdés*[b] and David Morales-Morales *[a]

Received 4th January 2026,
Accepted 30th January 2026

DOI: 10.1039/d6dt00012f

rsc.li/dalton

Caffeine and other purine bases are naturally occurring, inexpensive, and readily available heterocycles composed of a fused imidazole–pyrimidine framework, whose five-membered imidazole core corresponds to an N-heterocyclic carbene (NHC) precursor. These features make purine scaffolds ideal precursors for the design of metal-NHC ligands that combine biological relevance, structural diversity, and tunable electronic properties. Over the past two decades (2004–2025), an expanding family of purine-derived NHC complexes has been developed across the periodic table, including those of Ru, Ir, Rh, Ni, Pd, Pt, Cu, Ag and Au, revealing distinctive coordination modes, redox behaviors, and catalytic activities. This review provides a comprehensive overview of their synthetic strategies, structural features, and catalytic applications, emphasizing how the intrinsic anisotropy and multifunctionality of the purine framework enable unique metal–ligand interactions and reactivity patterns relevant to sustainable catalysis, photophysics, and bio-organometallic chemistry.

1. Introduction

The isolation of the first stable free carbene represents a seminal milestone in modern chemistry.[1–4] This achievement opened the way for the design of functionalized imidazolylidene scaffolds, later known as N-heterocyclic carbenes (NHCs), which rapidly emerged as powerful ligands in transition-metal

[a]Instituto de Química, Universidad Nacional Autónoma de México, 04510 Coyoacán, CDMX, Mexico. E-mail: alejandro.cervantes@iquimica.unam.mx, damor@unam.mx
[b]Departamento de Química Orgánica y Química Inorgánica, Instituto de Investigación Química "Andrés M. del Río" (IQAR), Facultad de Farmacia, Universidad de Alcalá, Alcalá de Henares, 28805 Madrid, Spain.
E-mail: hugo.valdes@uah.es

Alejandro Cervantes-Reyes

Dr Alejandro Cervantes-Reyes earned his Ph.D. (Magna Cum Laude) from Universität Heidelberg (2017–2020) mentored by Prof. A. Stephen K. Hashmi, specializing in ring-expanded NHC–coinage metal complexes for homogeneous catalysis. He then completed a postdoctoral stay (2021–2022) at Rutgers University (Newark, NJ) with Prof. Michal Szostak, working on palladium-catalyzed cross-couplings and NHC ligand design. Following his tenure as a Research Scientist at Paraza Pharma Inc. in Montreal (2022–2024), he returned to Mexico for a brief sabbatical. Since September 2024, he has been a DGAPA Postdoctoral Fellow at the Instituto de Química, UNAM, in the laboratory of Prof. David Morales-Morales, focusing on well-defined NHC–metal complexes for catalytic and medicinal applications.

Ricardo Malpica-Calderón

Ricardo Malpica-Calderón is a junior researcher currently pursuing his M.Sc. in Chemistry at the Instituto de Química, Universidad Nacional Autónoma de México (UNAM), under the guidance of Dr David Morales-Morales. He holds a B.Sc. in Chemistry from the Facultad de Química, UNAM (2023). His main research field is the design and study of transition-metal pincer and NHC–carbene complexes applied to the development of metallodrugs and catalysis used in the battle against cancer and the improvement of chemical transformations.

catalysis.[5–9] Since then, NHC–metal complexes have become an essential class of organometallic compounds, underpinning advances in selectivity control, catalytic efficiency, and reaction design across organic and inorganic chemistry.[10,11] Over the past decades, an extensive variety of structurally diverse NHC–metal architectures has been developed, fine-tuning steric and electronic properties to enable new reactivity pathways, enhance substrate scope, and provide cost-effective alternatives for industrially relevant transformations.[12–26]

Purines constitute an especially appealing platform within this landscape. These aromatic heterocycles consist of a fused pyrimidine–imidazole core, and naturally occurring derivatives, such as adenine, guanine, hypoxanthine, xanthine, theobromine, theophylline, isoguanine, and caffeine, exhibit rich tautomeric behavior arising from keto–enol and amine–imine equilibria.[27] Fig. 1 depicts the purine skeleton and its derivatives, highlighting the atom numbering scheme adopted throughout this review. The imidazole fragment within the purine structure inherently contains a pre-carbenic site (C8), which can be exploited for metal coordination, providing enhanced stability and tunable electronic environments in organometallic catalysis.[28] In some cases, an additional pre-carbenic position may also be available on the pyrimidine ring (C2). Related fused NHC scaffolds based on pyridine–imidazole frameworks have also been described in the literature.[29–60]

Among these, xanthine derivatives have attracted growing attention due to their natural abundance, low cost, and ready availability. These compounds serve as bio-derived NHC precursors, enabling the development of functionalized NHC–metal complexes suitable for both homogeneous and heterogeneous catalysis.[61–66] Their structural diversity allows for derivatization through straightforward *N*-alkylation or tether modification, yielding ligands with tailored solubility, steric bulk, and electronic profiles, and even surface-anchored catalysts when supported on materials such as graphene, silica, or polystyrene.

While several reviews have summarized the synthetic and biological aspects of purine-based NHC complexes,[67–69] their catalytic reactivity has often been only briefly mentioned or treated tangentially. To the best of our knowledge, no comprehensive review has yet focused specifically on the catalytic applications and reactivity studies of NHC–metal complexes derived from purine frameworks.

Hugo Valdés

Hugo Valdés completed his PhD degree with honors at Jaume I University in 2015 under the supervision of Prof. E. Peris and Dr M. Poyatos. Subsequently, he pursued postdoctoral studies in the group of Prof. D. Morales-Morales at the Institute of Chemistry, UNAM. Following this, he joined the group of Prof. X. Ribas at the University of Girona as a postdoctoral researcher under the Beatriu de Pinós Program. Recently, he started as an Assistant Professor at the University of Alcalá. His research interests revolve around the development of catalysts for C–C and C–heteroatom bond formation via C–H bond activation.

David Morales-Morales

Prof. Dr David Morales-Morales earned his BSc and MSc degrees from the Facultad de Química of the Universidad Nacional Autónoma de México (UNAM) and his PhD degree from the University of Essex, specializing in organometallic chemistry and catalysis. After a postdoctoral stay at the University of Hawaii at Manoa, he took his current position at the Instituto de Química, UNAM. His research interests include the chemistry of pincer compounds, the synthesis of phosphorus-, nitrogen- and sulfur-based compounds and their use as ligands with transition metals, metal-mediated organic synthesis, mechanistic studies, catalysis, and medicinal and green/sustainable chemistry. He has been part of the advisory board of the journal ChemCatChem and currently serves on the advisory board of the International Symposium on Homogeneous Catalysis (ISHC) and as an Associate Editor of Frontiers in Pharmacology and Frontiers in Chemistry, also serving as an editorial board member for the journals Inorganics (MDPI) and Discover Catalysis (Springer Nature). He has served as the editor of the books The Chemistry of Pincer Compounds (co-edited with C. M. Jensen, Elsevier, 2007) and Pincer Compounds. Chemistry and Applications (Elsevier, 2018). In 2024, he was designated Editor-in-Chief of the journal Applied Organometallic Chemistry (Wiley). He is a member of the Advisory Board of Dalton Transactions and was elected Fellow of the Royal Society of Chemistry (FRSC) in 2025.

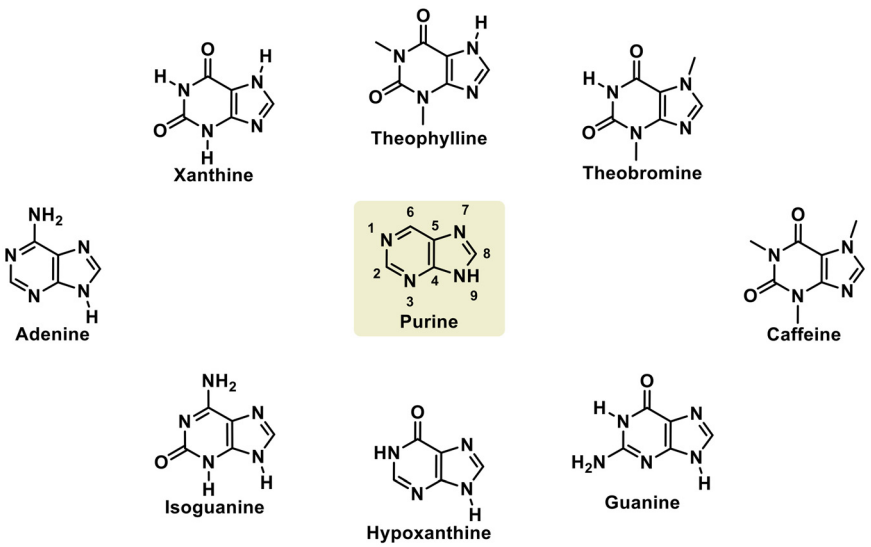

Fig. 1 Structure of purine and representative naturally occurring derivatives. The purine *core* features a fused pyrimidine–imidazole framework; atom numbering follows the scheme shown. Derivatives such as adenine, guanine, xanthine, theobromine, theophylline, and caffeine illustrate the structural diversity and functionalization patterns relevant to NHC precursor design.

In this contribution, we present an integrated overview (2004–2025) of the catalytic behavior of purine-derived NHC–metal complexes, encompassing Ru, Ir, Rh, Ni, Pd, Pt, Cu, Ag and Au systems. Special attention is given to their synthetic methodologies, ligand-transfer processes, ancillary-ligand exchange dynamics, and catalytic transformations, including cross-coupling, condensation, and hydrogen-transfer reactions. Through this analysis, we aim to establish purine-based NHC ligands as a sustainable and multifunctional platform in transition-metal catalysis, bridging the gap between bio-inspired design and advanced organometallic reactivity.

2. Purine-based NHC complexes of Group 8 metals

Group 8 of the periodic table comprises iron (Fe), ruthenium (Ru), and osmium (Os). In the literature, several Fe complexes incorporating a purine fragment have been reported.[70–76] However, to the best of our knowledge, there are no examples of Fe complexes featuring purine-derived NHC ligands, highlighting a clear gap in this area. Purine-based NHC complexes of Os[77] have been explored at the DFT level (B3LYP/6-311++G(d,p)//LANL2DZ), providing valuable theoretical insights into their bonding characteristics and electronic structure.[78]

In contrast to Fe and Os, some purine-based Ru–NHC complexes have been described in the literature, together with their catalytic applications.[79] In particular, xanthine-derived Ru(II)–NHC complexes **1a** and **1b** were evaluated in a series of transformations, including transfer hydrogenation, alkene oxidation, and the synthesis of vinyl ester compounds.[79] The transfer hydrogenation reaction was performed in i-propanol, which served simultaneously as a solvent and hydrogen donor (Scheme 1). Both complexes exhibited comparable catalytic performance, affording yields between 59% and 99% across various substrates. Remarkably, an imine substrate was quantitatively reduced to the corresponding secondary amine. This behavior is consistent with previous reports describing Ru-complex-mediated hydrogen transfers.[80]

The oxidation of alkenes using **1a** and **1b** (1 mol%) in the presence of $NaIO_4$ produced benzaldehyde and acetophenone selectively from styrene and methylstyrene, respectively, within 30–45 min (Scheme 2a). The formation of the corresponding carboxylic acids was not detected under these conditions. In contrast, oxidation of aliphatic substrates such as 1-hexene and cyclooctene afforded the corresponding carboxylic acids after 24 h in moderate to good yields (Scheme 2b).

Complexes **1a** and **1b** also catalyzed the formation of vinyl esters from benzoic acid and 1-hexyne under microwave irradiation. The reaction afforded mixtures of Markovnikov (using **1a**, yield: 72%, and **1b**, yield: 58%) and anti-Markovnikov (using **1a**, yield: 28%, and **1b**, yield: 42%) products. The distinct *Z*/*E* selectivities observed underscore marked differences in the reactivity and stereochemical behavior of the two Ru–NHC catalysts (Scheme 2c). Complex **1b**, bearing the bulkier *N*-substituent on the NHC ligand, favored the formation of the less sterically hindered *E*-stereoisomer.

The alkylation of anilines *via* dehydrogenative coupling represents a green and atom-economical strategy for C–N bond formation.[81] The methylation of aniline derivatives using methanol as a C1 source (Scheme 3) was accomplished through the *in situ* generation of a xanthine-based Ru–NHC complex (**2**).[82] This catalytic system exhibited good functional-group tolerance, accommodating halogens, ethers, and nitro

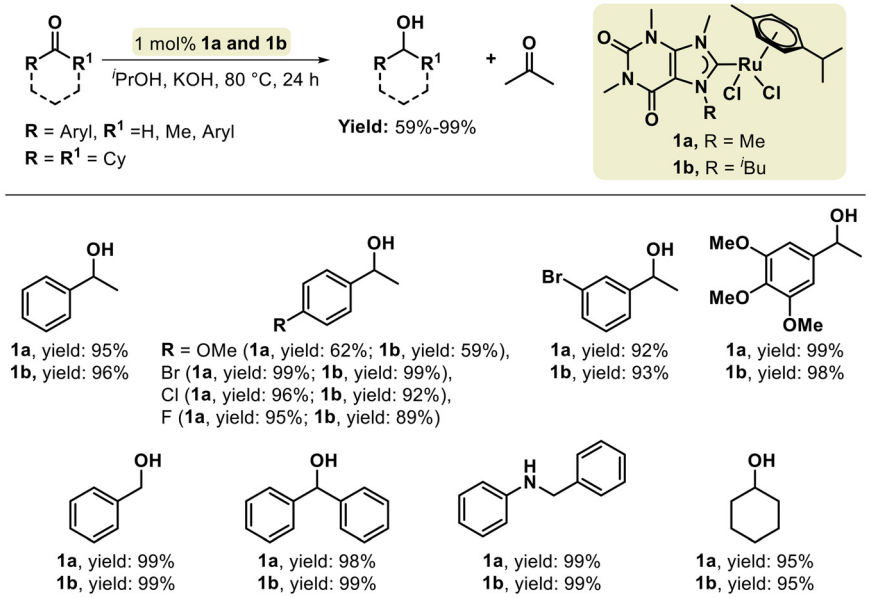

Scheme 1 Caffeine-derived Ru–NHC complexes (**1a** and **1b**) catalyze the transfer hydrogenation of ketones and a representative imine, affording the corresponding alcohols and secondary amine under mild conditions.

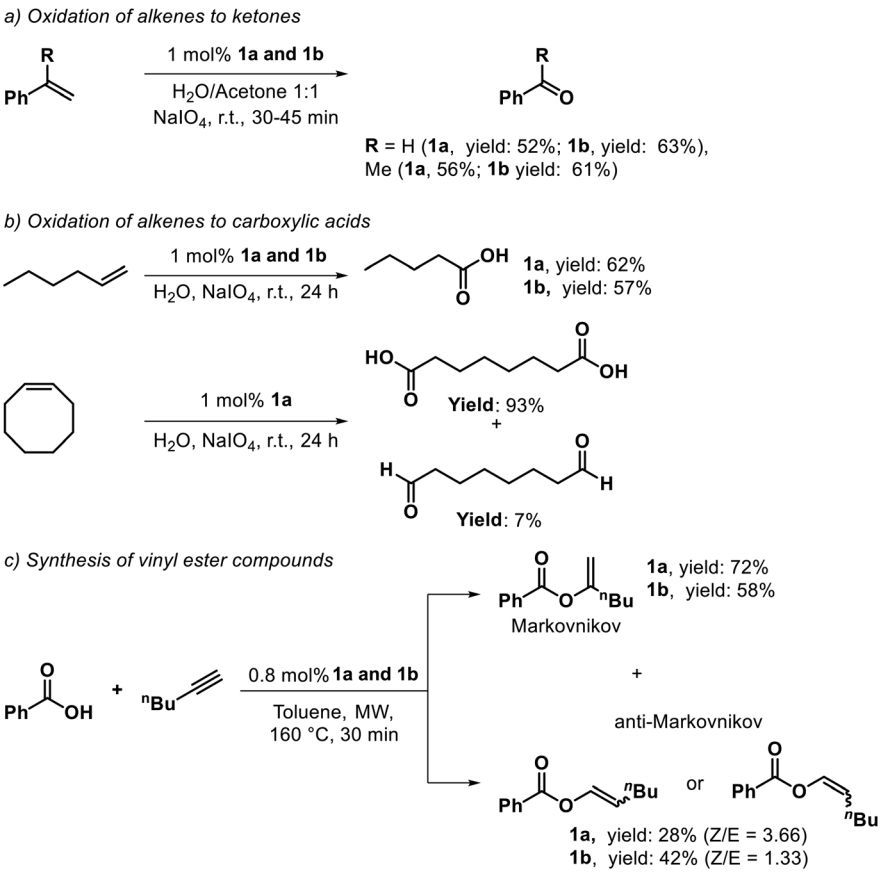

Scheme 2 Caffeine-derived Ru–NHC complexes (**1a** and **1b**) catalyze the oxidation of alkenes and the synthesis of vinyl esters, highlighting their versatility in redox and coupling transformations.

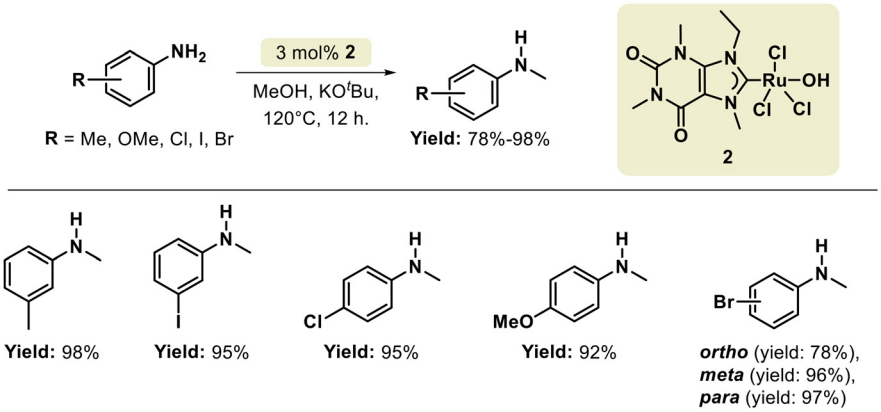

Scheme 3 NHC–Ru complex (**2**) catalyzes the dehydrogenative methylation of anilines with methanol, affording *N*-methylaniline derivatives under mild conditions.

substituents. Reported yields ranged from moderate to excellent (62–99%), highlighting the efficiency and versatility of the Ru–NHC framework.

The reactivity of Ru cluster **3** was examined in the presence of triphenylphosphine (Scheme 4).[77] At room temperature, cluster **3** reacted smoothly to afford the mono- and bis-phosphine-substituted derivatives $[Ru_3(CO)_9(PPh_3)\{\mu,\eta^1,\kappa^1\text{-}C_5N_4(CH_3)_3O_2\}(\mu\text{-H})]$ (**4a**) and $[Ru_3(CO)_8(PPh_3)_2\ \{\mu,\eta^1,\kappa^1\text{-}C_5N_4(CH_3)_3O_2\}(\mu\text{-H})]$ (**5**) in 38% and 8% yields, respectively. When the same reaction was performed in toluene under similar conditions, complexes **4a** and **5** were obtained in 41% and 21% yields, respectively. Both products are air-stable in the solid state, although they undergo slow decomposition in organic solution upon exposure to air. Attempts to obtain single crystals suitable for X-ray diffraction were unsuccessful. Cluster **4a** can undergo isomerization in solution through several pathways. For instance, migration of the PPh_3 ligand either to a second equatorial site on the same ruthenium center or to a different ruthenium center can generate a new isomer. Alternatively, hydride migration to another Ru–Ru edge may also lead to isomer formation. The two species likely differ by substitution at the nitrogen-bound ruthenium atom (major isomer) *versus* the carbon-bound ruthenium atom (minor isomer), as illustrated in Scheme 4b.

3. Purine-based NHC complexes of Group 9 metals

Over the past three decades, the chemistry of Group 9 metals has gained considerable attention owing to their broad catalytic versatility. Cobalt complexes containing a purine frag-

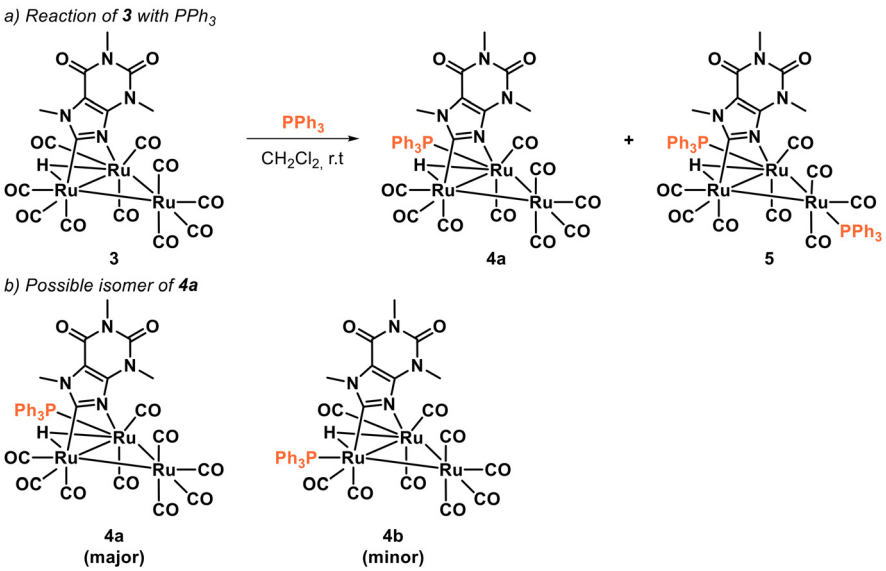

Scheme 4 Ligand exchange behavior of NHC–Ru complex **3** upon addition of PPh_3 and postulated structures of the two isomeric forms of the complex (**4a** and **4b**).

ment have been known since the 1950s.[75,76,83–89] However, to date, no examples of purine-derived NHC complexes of cobalt have been reported, despite the existence of numerous Co–NHC complexes in the literature with well-established catalytic applications.[90]

In contrast, several purine-based Ir–NHC complexes have been synthesized, characterized, and evaluated in catalytic transformations. The preparation of Ir(I)–NHC complexes of the type [(NHC)Ir(COD)Cl], where COD denotes 1,5-cyclooctadiene, has enabled their study from multiple perspectives. For example, the chloride ligand can be replaced by fluorinated arylthiolate (SAr^F) groups through ligand exchange with [Pb$(SArF)_2$],[91] which serves as a halide abstractor (Scheme 5). The driving force for this transformation is the formation of the insoluble [$PbCl_2$] byproduct and the strong affinity of Pb(II) for halide ions. The resulting Ir–SAr^F complexes (**7a** and **7b**) were isolated in 53% and 64% yields, respectively. Interestingly, incorporation of the SArF ligand enhanced cytotoxic activity but reduced selectivity; nevertheless, both complexes showed activity against several cancer cell lines, highlighting their potential as bioactive species.

The COD ligand in complexes of the type [(NHC)Ir(COD)Cl] can be readily substituted by CO,[92–94] affording the corresponding [(NHC)Ir$(CO)_2$Cl] species (Scheme 6).[66] This transformation is conveniently achieved by bubbling CO through a solution of the Ir–NHC precursor at 0 °C, a temperature that enhances CO solubility and promotes ligand exchange. The significance of the [(NHC)Ir$(CO)_2$Cl] complexes lies in the fact that their C–O stretching frequencies (ν(CO)) provide a direct measure of the electronic properties of the NHC ligand.[18,19,95–97] For complexes **8b–f**, the average ν(CO) values were 2019 cm^{-1} (**8a**), 2020 cm^{-1} (**8b** and **8c**), 2022 cm^{-1} (**8d**), and 2016 cm^{-1} (**8e**). Notably, the corresponding value for the well-known IMes derivative is 2023 cm^{-1},[97] serving as a useful benchmark for comparison.

A characteristic feature of Ir(III) complexes is their ability to activate C(sp^2)–H bonds, particularly when such activation enables the formation of five-membered metallacycles. This strategy has been extensively employed for the construction of bidentate ligands and their corresponding Ir(III) coordination

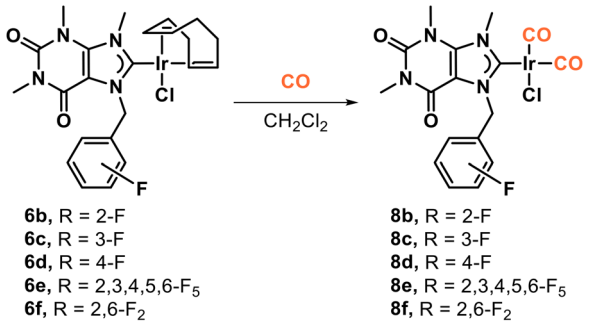

Scheme 6 Formation of dicarbonyl Ir–NHC complexes through CO substitution of the [(NHC)Ir(COD)Cl] precursor, illustrating ligand exchange from COD to CO.

compounds.[98] In this context, two structural isomers, **9-*mer*** and **9-*fac***, were isolated and fully characterized.[99] Remarkably, the *mer*-isomer can be converted into the *fac*-isomer upon treatment with trifluoroacetic acid (TFA) in a CH_2Cl_2/EtOAc mixture at 65 °C (Scheme 7). The two isomers display distinct photophysical properties, with quantum yields of 0.99 (**9-*mer***) and 0.77 (**9-*fac***), respectively.

Following a similar C(sp^2)–H activation strategy, a series of Ir(III) and Rh(III) complexes bearing C^D-chelating ligands (C = C8 of the purine *core*; D = C_{NHC}, NR_2 or PR_2) were synthesized.[100–102] In these systems, coordination of the metal to the D ligand precedes the C–H activation of the neutral purine, leading to the formation of an azolyl-type complex.[103–105] Subsequent protonation of the free nitrogen atom within the purine moiety affords access to the corresponding protic NHC (pNHC) species (Scheme 8).[100,101]

In the case of the xanthine–pyridine C^N chelate ligand (**10**), the ^{13}C NMR spectra of both complexes exhibit nearly identical chemical shifts for the C8 carbon—174.7 ppm for the pNHC complex (**11**) and 173.9 ppm for the azolyl analogue (**10**). This observation indicates that the C8 carbon functions as a carbene donor in both species, irrespective of the protonation state of the adjacent nitrogen atom.[100]

Coordination through the C2 position of the purine ring is also feasible (Scheme 9).[106] The reaction of caffeine with aqueous NaOH, followed by the sequential addition of concen-

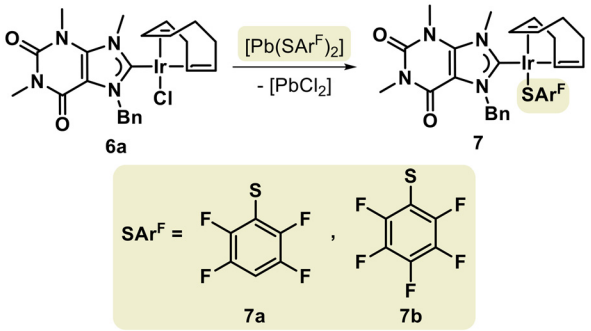

Scheme 5 Chloride-to-fluorinated arylthiolate ligand exchange in Ir–NHC complexes, illustrating the formation of SArF-substituted derivatives.

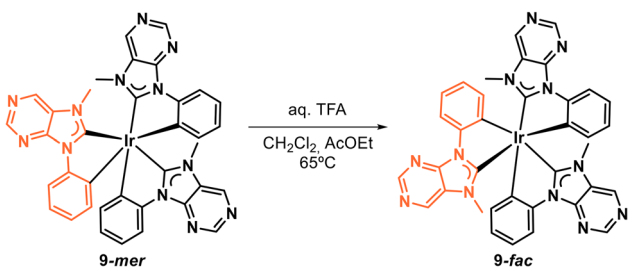

Scheme 7 Observed *mer*-to-*fac* isomerization of NHC–Ir complex **9** in acidic medium, illustrating reversible structural rearrangement under protonic conditions.

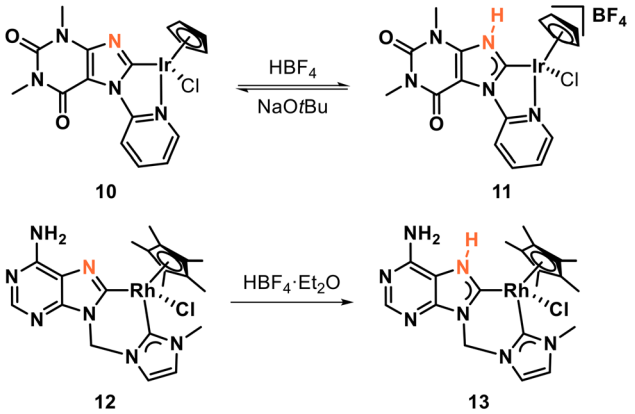

Scheme 8 Protonation of the free nitrogen atom within the purine moiety affords the corresponding protic NHC (pNHC) species.

trated HNO_3 and triethyl orthoformate [$HC(OEt)_3$], affords the corresponding azolium salt (**14**), which serves as a versatile precursor for the synthesis of Ir(I) and Rh(I) complexes. This azolium intermediate can also undergo C2–C2 dimerization, leading to the formation of a dimeric bis-NHC species (**16**), from which bis-NHC carbonyl Rh(I) complexes can be obtained (**17**). The Tolman electronic parameters (TEPs), determined from FT-IR spectra of the CO stretching bands, were 2057 cm^{-1} for the dimeric complex and 2058 cm^{-1} for the monomeric analogue, indicating comparable electron-donating abilities of the two NHC environments. Notably, these TEP values closely match those reported for NHC ligands bearing electron-withdrawing substituents directly attached to the heterocyclic backbone,[18] which is consistent with the presence of the carbonyl groups in the purine framework.

When two xanthine-derived NHC ligands are coordinated to the Rh(COD) fragment (**18**), the COD ligand can be readily replaced by carbon monoxide to yield the corresponding dicarbonyl complex **19** (Scheme 10).[107] The FT-IR spectrum displays two characteristic C–O stretching bands at ν(CO) = 2080 and 1962 cm^{-1}, consistent with a *cis*-configuration of the CO ligands. These relatively low frequencies reflect the strong σ-donor ability of the NHC ligands, which enhances back-donation from the metal center to the carbonyl groups.

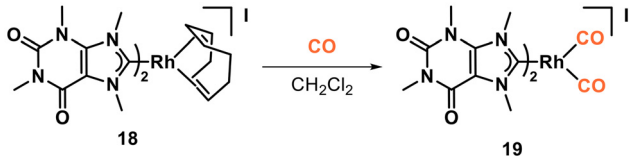

Scheme 10 Substitution of the COD ligand by CO in NHC–Rh complex **18**, yielding the corresponding dicarbonyl Rh-NHC species.

Iridium and rhodium complexes have been extensively investigated as catalysts in transfer hydrogenation, borylation, and hydroformylation reactions. In this context, some purine-based NHC complexes of Ir and Rh have been successfully applied in these transformations. Scheme 11 summarizes the reaction conditions and turnover numbers (TONs) reported for xanthine-derived Ir–NHC catalysts in transfer hydrogenation.[100,108–110]

Complex **20**, a caffeine-derived Ir–NHC species, exhibited notable catalytic activity in the transfer hydrogenation of ketones (Scheme 11a). The reaction, performed in the presence of KOH at 80 °C for 2 h, afforded TON values of up to 84.[108] In contrast, reactions catalyzed by the chelating Ir–NHC complexes **21a** and **21b** required significantly longer reaction times (30–90 h), achieving TON values of 33 and 13.3, respectively.[100]

The bis-NHC Ir complex **22** catalyzed the borylation of benzene through C(sp^2)–H activation, affording the corresponding product in a low yield (12%) (Scheme 11c).[109] The limited catalytic efficiency is likely attributable to the weak σ-donor character of the caffeine-derived NHC ligands, which reduces metal–ligand electron density. Furthermore, the non-chelating nature of the bis-NHC framework appears to disfavor the formation of the active Ir species after the initial catalytic turnover, thereby diminishing overall activity.

Rhodium complexes are widely employed as catalysts in the hydroformylation of olefins. The xanthine-derived Rh–NHC complex **23** effectively catalyzed the hydroformylation of 1-octene under high-pressure conditions (50 bar, CO/H_2 mixture) (Scheme 12).[110] After 1 h of reaction, a substrate conversion of 39% was achieved, corresponding to a turnover frequency (TOF) of 2410 h^{-1}. The linear-to-branched (l/b) aldehyde ratio at this stage was 1.5. As the reaction progressed and

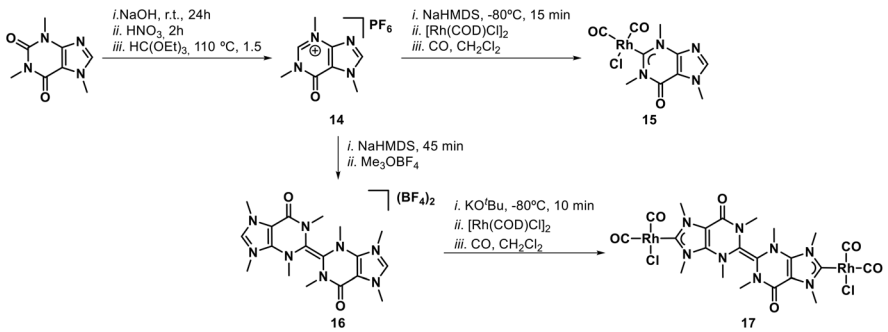

Scheme 9 Synthesis of dimeric Rh–NHC complex **16** and its Rh(I) carbonyl derivative.

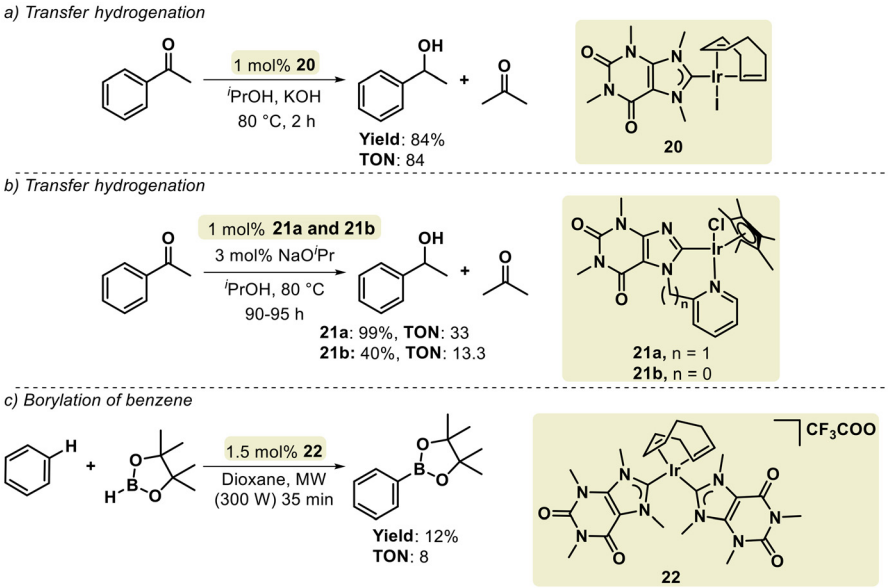

Scheme 11 Transfer hydrogenation and benzene borylation catalyzed by xanthine-based Ir–NHC complexes.

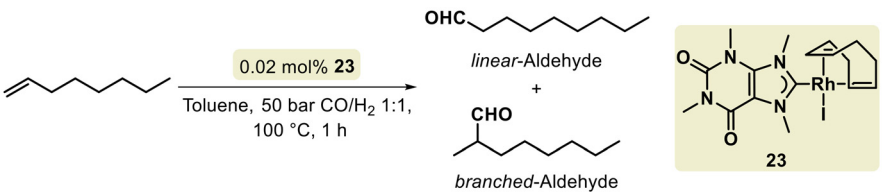

Scheme 12 Hydroformylation of 1-octene catalyzed by xanthine-based Rh–NHC complex (**23**).

the conversion increased to 80%, the l/b ratio decreased to 0.5, indicating that the branched aldehyde was formed preferentially as the kinetic product.

4. Purine-based NHC complexes of Group 10 metals

Group 10 metals are well known for their pivotal role in cross-coupling catalysis, particularly nickel and palladium, which have been extensively employed in a wide range of C–C and C–heteroatom bond-forming reactions.[111–120] Platinum, on the other hand, has found important applications in hydrosilylation of alkynes in aqueous media, where it acts as an active and recyclable catalyst, as well as in hydroamination reactions, which constitute key steps in the synthesis of nitrogen-containing heterocycles.[121–123] In addition, several Pt complexes have been explored as anticancer metallodrugs, expanding the relevance of Group 10 chemistry beyond catalysis.[124]

The Ni–NHC complexes (**24a–c**), stabilized by xanthine-derived ligands and a cyclopentadienyl ancillary group, were evaluated as catalysts in the Suzuki–Miyaura cross-coupling between aryl bromides and arylboronic acids (Scheme 13).[125] The catalytic scope was assessed using complex **24a**, which delivered 15 examples with yields ranging from 73% to 98%. Notably, **24a** also exhibited good activity in the coupling of aryl chlorides—in place of aryl bromides—when PPh_3 (5 mol%) was used as a co-ligand, affording biaryl products derived from pharmaceutical substrates such as chlorpromazine (81% yield), fenofibrate (73% yield) and indomethacin (82% yield).

Interestingly, complex **24c** is among the few reported examples in which a phenyl group is directly bonded to the N atom of the NHC ligand. Its synthesis is not straightforward and is typically achieved *via* an Ullmann coupling.[125,126] The presence of the phenyl substituent impacts the percent buried volume (%V_{bur}) of the NHC ligand. %V_{bur} is defined as the percentage of a sphere (r = 3.5 Å) centered at the metal that is occupied by the ligand.[127] For NHCs bearing *N*-methyl substituents, %V_{bur} is 27.8% (as in **24a**), whereas the introduction of an *N*-phenyl group increases this value to 31.2% (as in **24c**). NHC ligands featuring *N*-benzyl substituents display a slightly higher %V_{bur} of 32.3% (as in **24b**), consistent with the greater steric demand imposed by bulkier *N*-substituents around the metal center.

A graphene (GP)-supported, caffeine-derived Ni-NHC catalyst (**25**) efficiently promoted the arylation of benzoxazole with a broad range of arylboronic acids, affording a representative series of 2-arylbenzoxazoles (Scheme 14).[128] Under optimized

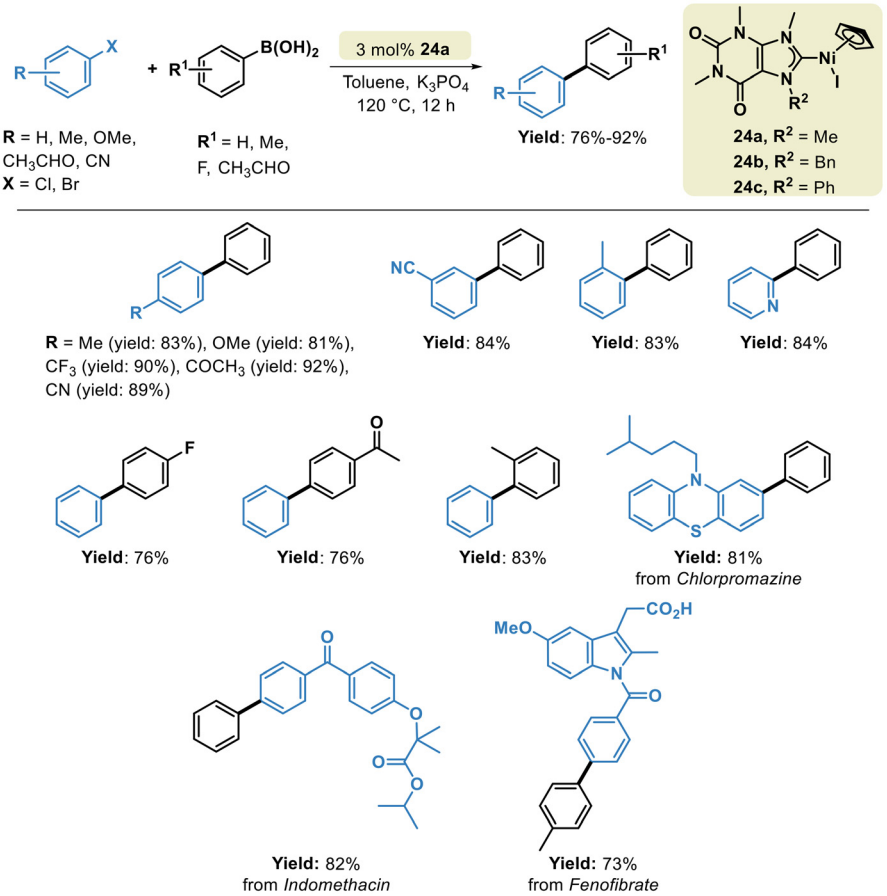

Scheme 13 Suzuki–Miyaura cross-coupling reaction catalyzed by xanthine-based Ni(II)–NHC complexes.

conditions, benzoxazole reacted with electron-deficient arylboronic acids, such as 4-nitrophenylboronic acid and 3,5-dichlorophenylboronic acid, to give the corresponding products, with yields of up to 78%. Reaction with neutral phenylboronic acid provided the corresponding product in 88% yield. Notably, arylation also proceeded efficiently with heteroarylboronic acids, including 3-thienylboronic acid and 2-furanylboronic acid, affording 87% and 84% yields, respectively.

NHC–palladium complexes are among the most prominent catalysts in modern organic synthesis. In particular, Pd–NHC pre-catalysts are highly versatile and efficient for promoting C–C and C–N cross-coupling as well as carbopalladation reactions, making them fundamental tools in both synthetic chemistry and homogeneous catalysis. The strong Pd–carbene bond endows these complexes with remarkable thermal and chemical stability, ensuring sustained activity of the catalytically relevant Pd(0) species even at low catalyst loadings. Moreover, the rational design of NHC ligands provides the necessary stereoelectronic protection to the metal center, suppressing undesired off-cycle Pd(I) species and maintaining high turnover efficiency.[111–113]

Under optimized conditions, Pd–NHC complexes enabled the efficient synthesis of structurally diverse molecules, ranging from fine chemicals to pharmaceuticals. Indeed, the development of palladium-catalyzed cross-coupling reactions represents a milestone in catalysis—an achievement recognized by the 2010 Nobel Prize in Chemistry, awarded to Richard F. Heck, Ei-ichi Negishi, and Akira Suzuki.[129]

In this context, purine-derived NHC–Pd complexes have recently emerged as innovative and efficient catalytic systems. Scheme 15 illustrates xanthine-based Pd(II) complexes that have been employed as catalysts in Suzuki–Miyaura C–C cross-coupling reactions.[130–136] Representative examples include reactions where an aryl halide or aryldiazonium salt serves as the electrophilic partner, while phenylboronic acid acts as the nucleophilic coupling reagent. Owing to the polar nature of xanthine ligands, most reported protocols utilize polar solvents—typically water, alcohols (i-propanol or methanol), or THF/water mixtures. The most commonly used bases are K_2CO_3 and KOH; however, when aryldiazonium salts are employed, the coupling can proceed efficiently under base-free conditions. Temperature also plays a key role, with most reactions being carried out between room temperature and 100 °C, depending on substrate reactivity and catalyst loading.

One of the main advantages of xanthine derivatives is their synthetic versatility, as they can be readily obtained from caffeine, theophylline, or theobromine. The N1, N7, and N9 positions of the xanthine core can be conveniently functiona-

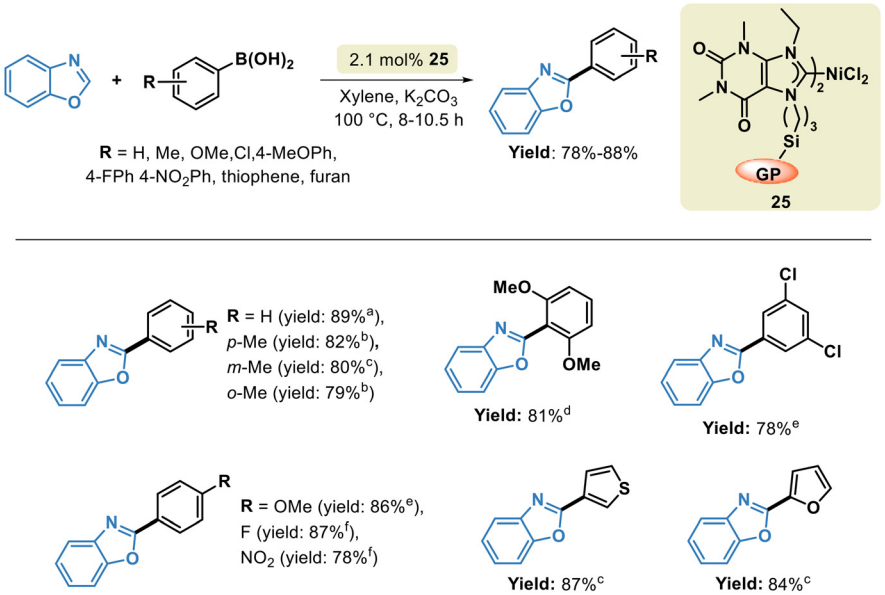

Scheme 14 Benzoxazole arylation reaction promoted by graphene-supported NHC–Ni complex (**25**). Arylboronic acid-dependent reaction times: [a] 8 h, [b] 8.5 h, [c] 9 h, [d] 10.5 h, [e] 9.5 h and [f] 10 h.

lized *via* nucleophilic substitution using alkyl halides, enabling straightforward ligand diversification. Complex **26** represents a bis-NHC species derived from caffeine, whereas in complexes **27a** and **27b**, the N1 and N9 nitrogen atoms were functionalized with methyl or benzyl (Bn) groups, respectively.

Such nitrogen functionalization provides an efficient means to tune the physicochemical properties of the resulting metal complexes or to anchor them onto supports. For instance, complex **31**, bearing a sulfonate substituent, exhibits enhanced water solubility and can be further immobilized on a nano-magnetite support, allowing easy recovery using an external magnet. Another noteworthy example is complex **32**, which was supported on a polystyrene matrix, demonstrating the versatility of xanthine-derived NHC frameworks for heterogeneous catalysis.

A wide variety of co-ligands can be incorporated around the metal center, providing additional stability and functional diversity. Typical examples include halides, acetates, heterocycles, phosphines, and allyl ligands. The water solubility of complexes **27a–c**, for instance, was significantly enhanced by coordination of the sodium triphenylphosphine trisulfonate (TPPTS) ligand, a well-known hydrophilic phosphine. Moreover, the formation of PEPPSI (Pyridine Enhanced Precatalyst Preparation, Stabilization and Initiation)-type complexes is also feasible within this family. Such PEPPSI-NHC systems are generally recognized as highly active and robust catalysts, combining excellent air stability with efficient palladium(II) reduction under catalytic conditions.

A direct comparison of the catalytic activity of the various xanthine-based Pd–NHC complexes is not straightforward, as they have been evaluated under different reaction conditions. Nevertheless, several consistent trends can be identified. Complexes **26**, **27**, **28**, **29**, **31**, and **30** displayed notable activity in the Suzuki–Miyaura coupling of a broad range of aryl bromides. Among them, the PEPPSI-type complexes exhibited the highest turnover numbers (TONs), reaching values of up to 380 for complex **28b**. Substrates containing electron-withdrawing groups (EWGs), such as $-NO_2$, –CHO, –COR, and $-CF_3$, generally provided higher yields than those bearing electron-donating groups (EDGs), including –OH, –OMe, and –alkyl. This behavior reflects the facilitating influence of EWGs on the oxidative addition step, which promotes palladium insertion into the C–Br bond and thereby accelerates the catalytic cycle.

The nature of the aryl halide also exerts a significant influence on catalytic performance. As expected, aryl iodides generally exhibit higher reactivity than aryl bromides, consistent with the well-established order of oxidative addition rates (I > Br > Cl) for palladium-catalyzed cross-coupling reactions. Notably, among the xanthine-derived catalysts, only complex **31** exhibited measurable activity toward the more challenging aryl chlorides, delivering the biphenyl product in 80% yield.

In contrast, aryl diazonium salts undergo oxidative addition much more readily than halides, owing to nitrogen gas evolution, which acts as a strong thermodynamic driving force. Using complex **32a**, cross-coupling products were obtained in 58–98% yields under base-free conditions and at room temperature, underscoring the excellent activity of purine-based Pd–NHC catalysts toward diazonium substrates.

Halogenated heterocycles were also evaluated as substrates in cross-coupling reactions. For instance, complex **27c** efficiently catalyzed the Suzuki–Miyaura coupling of 2-bromothiophene, affording the desired product in 40% yield at 60 °C. Increasing the reaction temperature to 80 °C markedly improved the yield to 95%. In another example, complex **29a**

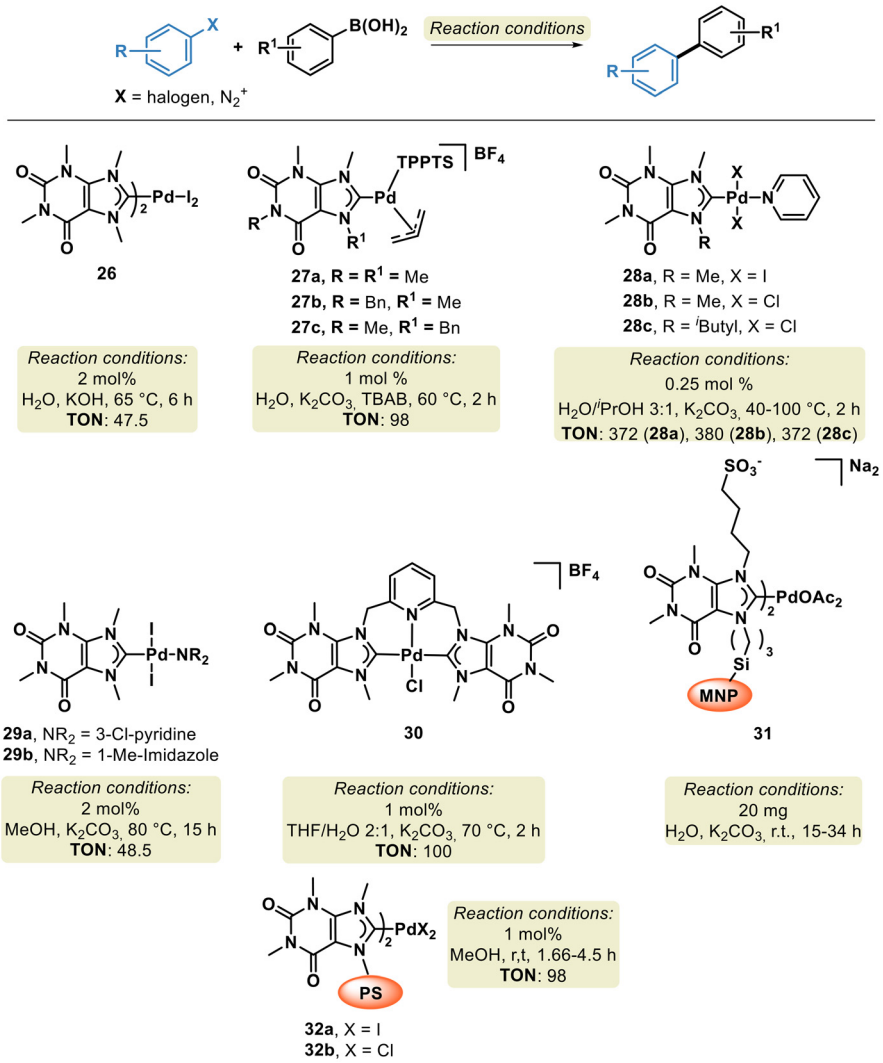

Scheme 15 Xanthine-based NHC-Pd(II) complexes catalyze Suzuki–Miyaura cross-coupling reactions.

successfully promoted the coupling of 3-bromopyridine, delivering the corresponding product in 97% yield, thus demonstrating the broad substrate tolerance of xanthine-based Pd–NHC catalysts toward heteroaryl bromides.

Complexes **28a**, **29a** and 29**b** were also evaluated as catalysts in cross-coupling between *N*-benzoylglutarimide and arylboronic acids (Scheme 16).[133] The reactions were conducted using 2 mol% of catalyst in 1,4-dioxane as the solvent, with K_2CO_3 as the base, at 120 °C for 15 h. All three complexes displayed comparable catalytic activity, affording the coupling products in 75% (**28a**), 76% (**29a**), and 81% (**29b**) yields, with corresponding TONs of 37.5, 38.0, and 40.5, respectively.

Another representative transformation catalyzed by palladium complexes is the Heck-type reaction. Scheme 17 summarizes the catalysts that have been employed for this purpose and the corresponding reaction conditions.[130,133,135,137] A wide range of solvents have been explored for this transformation, most of which are polar media. Typical examples include water, ethanol, i-propanol, *N*-methylpyrrolidone (NMP), and dimethylacetamide (DMA). The base of choice is generally

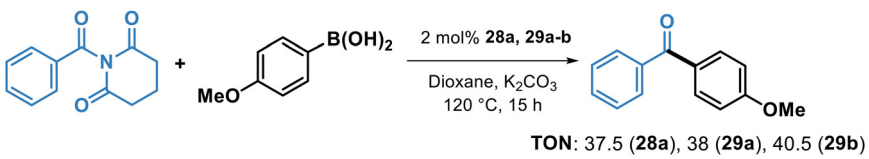

Scheme 16 Cross-coupling between *N*-benzoylglutarimide and arylboronic acids catalyzed by the Pd–NHC complex.

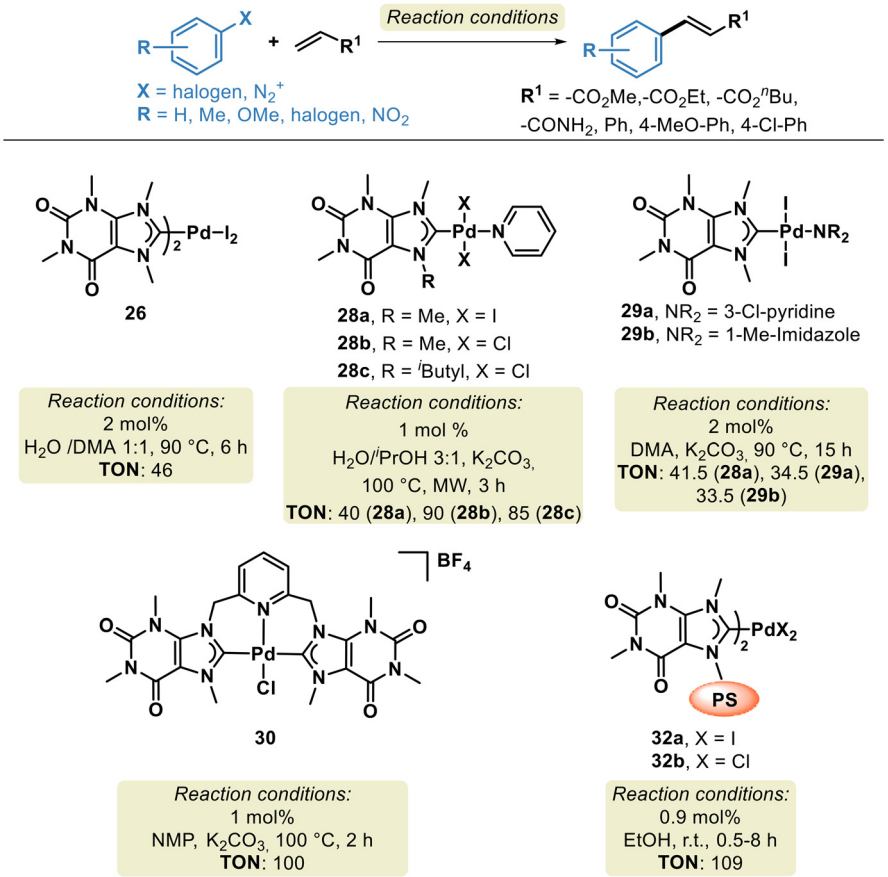

Scheme 17 Xanthine-derived NHC–Pd(II) complexes **26**, **28a–c**, **29a**, **29b**, **30**, and **32a** reported as catalysts for Heck-type cross-coupling reactions. Representative conditions are summarized, typically relying on polar media and K_2CO_3 as the base at 90–100 °C, although base-free variants have been described. Complex **32a** has also been applied to Heck-type couplings of aryl diazonium salts under mild conditions at room temperature.

K_2CO_3, although an example has been reported under base-free conditions. The reactions are typically conducted at temperatures between 90 and 100 °C.

Complexes **28a–c**, **29a**, **29b**, and **30** efficiently catalyzed Heck-type coupling reactions using aryl bromide substrates, whereas complex **26** was active with aryl iodides at 90 °C. The corresponding turnover numbers (TONs) were 46 (**26**), 40 (**28a**), 90 (**28b**), 85 (**28c**), 41.5 (**28a**), 34.5 (**29a**), 33.5 (**29b**), and 100 (**30**), respectively. As expected, the use of aryl chlorides remains challenging. However, complex **30** was capable of catalyzing reactions involving aryl chlorides bearing electron-withdrawing groups (EWGs), which facilitate C–Cl bond activation. For example, the cross-coupling of methyl acrylate with 1-iodo-4-nitrobenzene afforded the Heck-type product in 20% yield, while the corresponding bromide or iodide substrates produced the product in quantitative yield (100%). In contrast, substrates containing electron-donating groups (EDGs) negatively affected the reaction efficiency; in the case of 4-bromoanisole catalyzed by complex **30**, the yield decreased to 25%.

Complex **32a** efficiently catalyzed the Heck-type reaction using aryl diazonium salts as substrates at room temperature, achieving a TON of 109. This methodology exhibited broad olefin tolerance, accommodating a wide variety of substituents such as $-CO_2Me$, $-CO_2Et$, $-CO_2{}^nBu$, $-CONH_2$, –Ph, *p*-methoxyphenyl, and *p*-chlorophenyl groups.

Complexes **28a–c** efficiently catalyzed the coupling of 1-methyl-2-pyrrolecarboxaldehyde and 3,5-dimethylisoxazole with a variety of aryl bromides.[137] The reactions were carried out under conditions analogous to those employed in Heck-type couplings, using 1 mol% of catalyst, potassium acetate as the base, and DMA as the solvent at 120 °C for 4 h (Scheme 18).

When 1-methyl-2-pyrrolecarboxaldehyde was used as the substrate, the turnover numbers (TONs) reached 65 for **28a**, 94 for **28b**, and 85 for **28c**. In contrast, reactions with 3,5-dimethylisoxazole afforded slightly lower TON values of 46 (**28a**), 61 (**28b**), and 69 (**28c**). The reaction conditions exhibited good functional-group tolerance, accommodating aldehyde (CHO), ketone, and methoxy (OMe) substituents without noticeable deactivation.

Xanthine-based Pd–NHC complexes also exhibit catalytic activity in the Sonogashira cross-coupling reaction. Complexes **26**, **28a**, **29a**, **29b** and **30** effectively catalyzed the transformation (Scheme 19) at temperatures between 90 and 100 °C.[130,133,135] The TONs obtained for the different catalysts were 48 (**26**), 40 (**28a**), 41 (**29a**), 49 (**29b**), and 100 (**30**). As

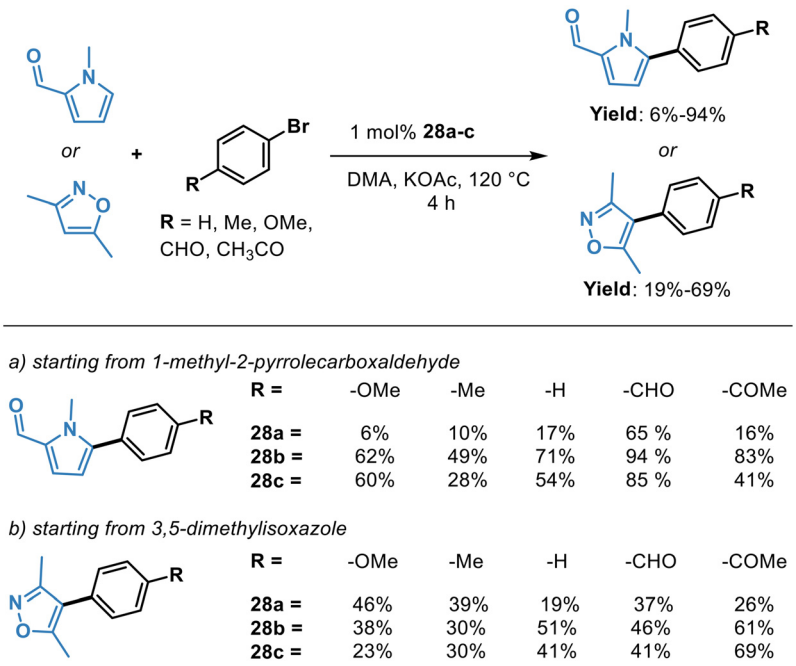

R =	-OMe	-Me	-H	-CHO	-COMe
28a =	6%	10%	17%	65 %	16%
28b =	62%	49%	71%	94 %	83%
28c =	60%	28%	54%	85 %	41%

R =	-OMe	-Me	-H	-CHO	-COMe
28a =	46%	39%	19%	37%	26%
28b =	38%	30%	51%	46%	61%
28c =	23%	30%	41%	41%	69%

Scheme 18 Cross-coupling of 1-methyl-2-pyrrolecarboxaldehyde and 3,5-dimethylisoxazole with aryl bromides catalyzed by NHC–Pd complexes **28a–c**.

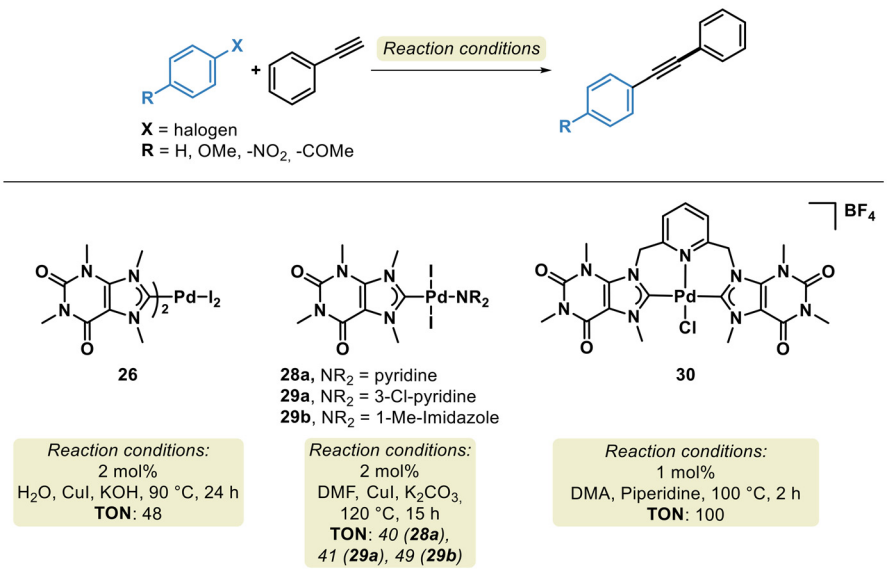

Scheme 19 Xanthine-based NHC–Pd(II) complexes catalyze Sonogashira cross-coupling reactions.

expected, pincer complexes are well-recognized for their high catalytic robustness and stability, which explains the superior performance of complex **30** in this transformation.

A series of caffeine-derived Pd–NHC catalysts were evaluated in the cyanation of aryl bromides (Scheme 20).[138] Preliminary studies revealed that the zwitterionic complexes (**33c**, **33e**, and **33g**) were significantly more active, affording up to 99% yield after 4 h, compared to their chelated counterparts (**33a**, **33b**, and **33d**), which produced up to 50% yield. This enhanced reactivity is presumably due to the anionic substituent in the zwitterionic species, which improves the solubility of the active Pd–NHC intermediates in the aqueous reaction medium. Further exploration of the reaction scope using complexes **33f** and **33g** as catalysts afforded a broad range of products, with yields of 12–64% (**33f**) and 16–74% (**33g**) and corresponding TON values of 64 and 74, respectively, under similar conditions.

On the other hand, bis(pNHC) Pd(II) complexes can also be obtained.[139] These species exhibit a dynamic equilibrium

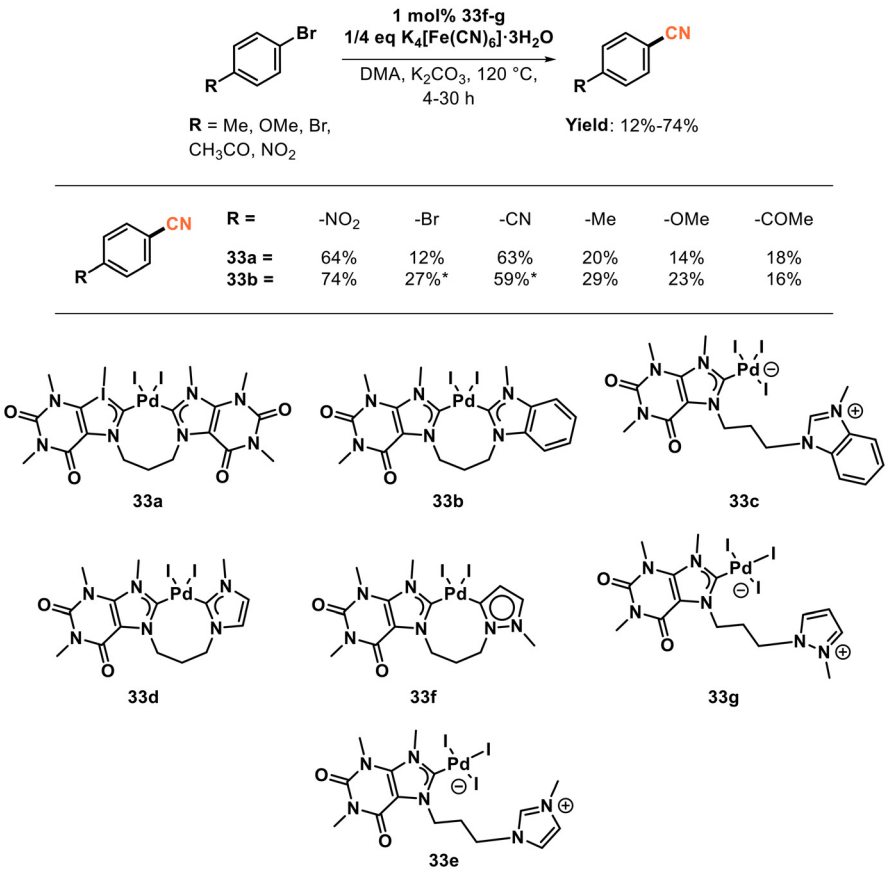

Scheme 20 Xanthine-based NHC–Pd(II) complexes catalyze cyanation of aryl halides.

between the bis(pNHC) complex (**34**) and the 'theophyllinate' complex (**35**), in which the theophylline ligand coordinates through the N9 atom. In this system, the pNHC form corresponds to the kinetic product, whereas the 'theophyllinate' species represents the thermodynamic product, as illustrated in Scheme 21. This equilibrium is solvent-dependent: the 'theophyllinate' complex is favored in poorly coordinating solvents (*e.g.*, $CDCl_3$), where the carbene species is almost undetectable by ^{13}C NMR spectroscopy. Conversely, in strongly coordinating solvents such as DMSO-d_6, the NHC form is stabilized and can be clearly identified spectroscopically.

Purine-based NHC complexes of platinum have also been synthesized.[105,140–142] However, to the best of our knowledge, no catalytic applications have been reported to date. Instead, these Pt–NHC systems have primarily been explored for their biological properties, including potential anticancer activity.[67,140,142]

5. Purine-based NHC complexes of Group 11 metals

The chemistry of Group 11 metals (Cu, Ag, and Au) is highly distinctive for each element. Copper, one of the most abundant transition metals in the Earth's crust, occurs mainly in mineral ores and is commonly commercialized as sulfate, carbonate, halide, or oxide salts. These compounds are benchstable, inexpensive, and readily available—qualities that make copper an attractive metal feedstock for catalyst preparation and other industrial applications.[118,143,144]

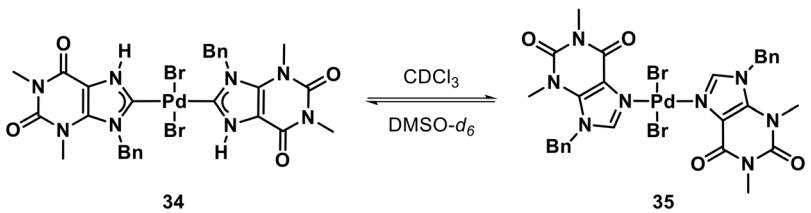

Scheme 21 Dynamic equilibrium between NHC–Pd complexes **34** and **35**.

Cu–NHC complexes are particularly well established in σ-/π-activation reactions involving molecules with multiple bonds (*e.g.*, olefins, alkynes, NH_3, and CO_2), typically enabling functionalization and heteroatom incorporation, or even C–H bond activation. A notable example is the copper-catalyzed alkyne–azide cycloaddition ("click reaction"), which affords 1,4-disubstituted 1,2,3-triazoles with complete atom economy.[25,145–150]

In contrast, silver and gold are far less abundant and are classified as precious transition metals. Although their catalytic applications have been known for decades, the last two to three decades have witnessed a resurgence of interest, particularly due to their ability to act as mild Lewis acid catalysts.[151–156] The following sections summarize the coordination chemistry, catalytic behavior, and reactivity trends of Group 11 metal complexes bearing purine-derived NHC ligands.

The theophylline-based Cu(I)–NHC complex (**36**), incorporating a hydrophilic ammonium salt unit, was evaluated as a catalyst for regioselective alkyne–azide cycloaddition between alkynes and alkyl halides in aqueous medium (Scheme 22).[64] Under these conditions, a representative library of 1,4-disubstituted 1,2,3-triazoles was obtained in yields of up to 93%.

The catalytic activity of complex **36** was also examined in the Glaser homocoupling of alkynes (Scheme 23),[64] affording 1,3-diynes in moderate to good yields (73–92%). The catalyst exhibited good substrate tolerance, efficiently converting diversely substituted alkynes, although electron-donating substituents appeared to enhance reaction efficiency. Recyclability experiments revealed certain limitations in catalyst recovery and reuse; however, the use of a catalyst based on inexpensive copper and a naturally occurring theophylline-derived NHC ligand represents a valuable advance toward sustainable, water-mediated Cu catalysis.

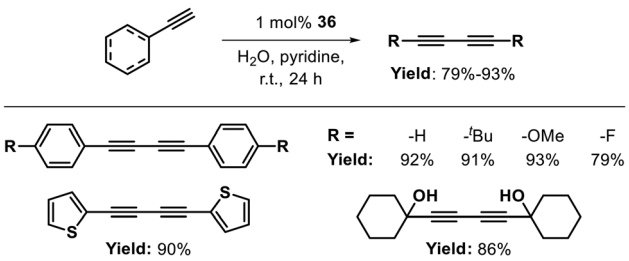

Scheme 23 Glaser homocoupling of alkynes catalyzed by Cu(I)–NHC complex **36**.

The cellulose/alumina (C/A)-supported Cu complex (**37**), derived from a caffeine-based NHC ligand, efficiently promoted the Ullmann-type coupling for the synthesis of diaryl ethers (Scheme 24).[157] The reaction employed either phenyliodide or phenylbromide as aryl halide partners, together with a library of phenols bearing substituents of varying electronic and steric characteristics. When phenyliodide was used as the substrate, the reaction afforded slightly higher yields (71–90%) compared to the bromide analogues (64–83%). Notably, the presence of electron-withdrawing substituents (*e.g.*, R = NO_2) had a negative effect on the reaction outcome, resulting in lower yields (64–69%).

Caffeine-based NHC complexes of silver (**38a–c**) and gold (**39a–c** and **40**), featuring *N*-attached hydroxyethyl-substituted

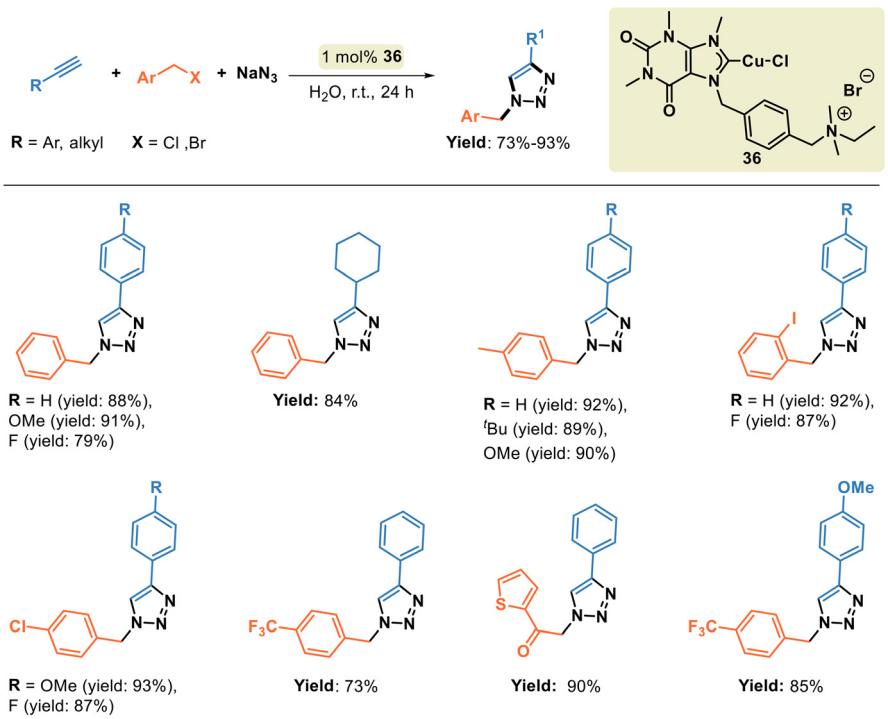

Scheme 22 Alkyne–azide cycloaddition ("click reaction") catalyzed by Cu(I)–NHC complexes.

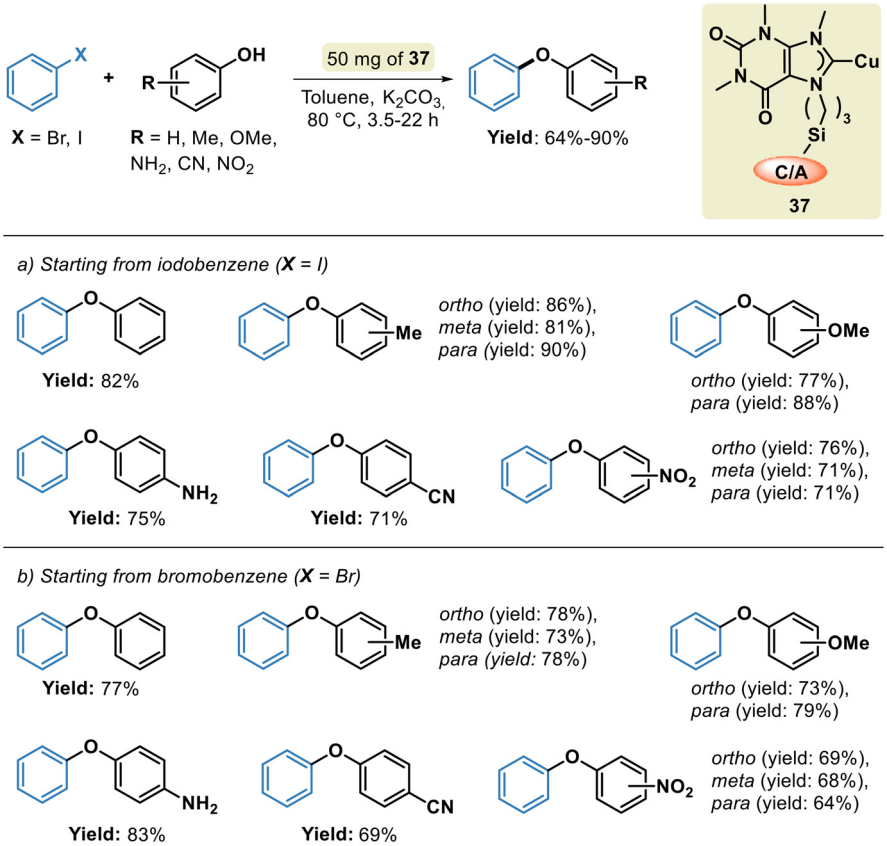

Scheme 24 Ullmann-type coupling catalyzed by Cu(I)–NHC complex **37**.

wingtips, were evaluated as catalysts in the synthesis of propargylamines (Scheme 25a) and the hydroamination of alkynes (Scheme 25b).[158] In the propargylamine synthesis (15–99% yield), the catalytic activity showed a marked dependence on the nature of the aldehyde. For instance, the [Ag(NHC)OAc] complex (**38a**) afforded 95% yield when acetaldehyde was used as the substrate, whereas the yield dropped sharply to 15% with benzaldehyde, highlighting a strong aromatic substituent effect.

Similarly, the gold acetate analogue (**40**) provided 91% yield with acetaldehyde, but only 54% yield with benzaldehyde, a trend consistent across a series of Au–NHC complexes. Furthermore, catalyst **40** was successfully applied to the hydroamination of alkynes, producing four different imine derivatives in moderate yields (39–73%). These results emphasize the Lewis-acidic character of Ag(I) and Au(I) centers, which plays a crucial role in activating π-bonds and facilitating nucleophilic addition processes in such transformations.

Up to this point, we have discussed reactions catalyzed by Ag(I) in which the metal fragment acts primarily as a Lewis acid. More challenging catalytic transformations, where Ag participates in oxidative addition steps, have been reported for the caffeine-derived complex **41**. The polymer-supported (PS) complex **41** was evaluated in the Sonogashira coupling between terminal alkynes and aryl halides (Scheme 26).[159] The reaction scope revealed a representative library of non-symmetrical internal alkynes bearing various (hetero)aryl substituents, affording yields ranging from 54% to 92%. No clear trends related to electronic or steric effects were observed—for instance, R = H (63% yield), *p*-CHO (69%), *p*-OH (58%), and *o*-CHO (54%). This study represents one of the few examples in which oxidative addition at Ag(I) is achieved without the assistance of multidentate or fluorinated ligands,[160–174] underscoring the unique reactivity of the caffeine-based Ag–NHC system.

Collectively, these examples underscore that purine-derived coinage–metal NHC complexes can display reactivity that goes beyond simple Lewis-acid activation. In this context, the gold system below illustrates how Au–NHC connectivity may undergo slow, solvent-dependent reorganization under basic conditions. In the preparation of the NHC–Au complex (**42**), prolonged stirring of the bis-NHC proligand with [AuCl(SMe$_2$)] and K_2CO_3 in acetonitrile led to the formation of complex **43** (Scheme 27).[175] The synthesis of complex **42** proceeds at room temperature within 3 h, whereas the subsequent transformation into complex **43** requires 72 h for completion. The initial step corresponds to a ligand-transfer reaction, while the formation of **43** involves partial cleavage and reformation of the Au–NHC bond. This process appears to be solvent-dependent, as the coordinating ability of acetonitrile likely facilitates reorganization within the metal coordination sphere over time.

A key reactivity feature of NHC–Ag complexes lies in the lability of the C(NHC)–Ag bond, which can readily dissociate

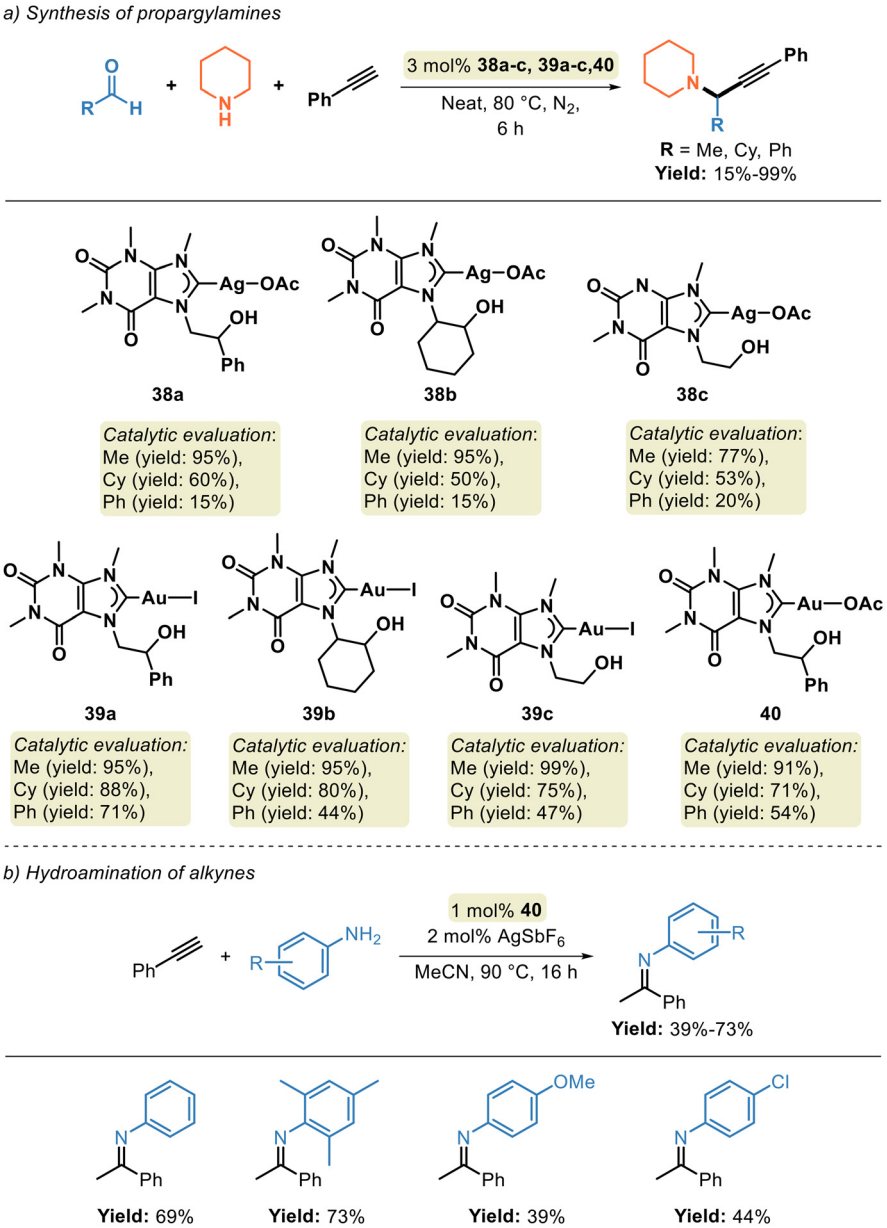

Scheme 25 Synthesis of propargylamines and hydroamination of alkynes catalyzed by Au– and Ag–NHC complexes.

in solution to establish dynamic equilibria among various silver species, the counteranion (*e.g.*, Cl^- and OAc^-), the free NHC ligand, and other $[NHC–Ag]^+_n$ fragments. This ligand-transfer reactivity is widely exploited as a synthetic route to other NHC–metal complexes, as it avoids the need for strong deprotonating agents, contaminant bases, or the isolation of free carbenes. The irreversible precipitation of AgX serves as the thermodynamic driving force, enabling clean isolation of the desired NHC–metal complex after filtration and solvent removal.[176–179]

This silver-mediated transmetalation strategy has been widely employed to prepare various NHC complexes, including those derived from xanthine ligands. For instance, rhodium and ruthenium NHC complexes (**44** and **1a**) were synthesized *via* a one-pot, two-step procedure involving the *in situ* activation of the corresponding xanthium triflate or iodide salts with $[Ag_2O]$, followed by transmetallation of the *in situ*-generated silver NHC intermediates with $[RhCl(COD)]_2$ or $[RuCl_2(p\text{-cymene})]_2$, respectively, to afford the final NHC–Rh and NHC–Ru complexes (**44** and **1a**) (Scheme 28a and b).[79,180,181] Notably, omitting the isolation of the intermediate silver NHC complex and directly introducing the target metal precursor into the reaction mixture proved equally effective, confirming the efficiency and general applicability of this ligand-transfer methodology.

The reaction of equimolar amounts of the NHC–Ag complex (**45**) and $[Rh(COD)Cl]_2$ in DMSO afforded the corresponding cationic NHC–Rh complex (**46**) *via* a typical ligand-transfer

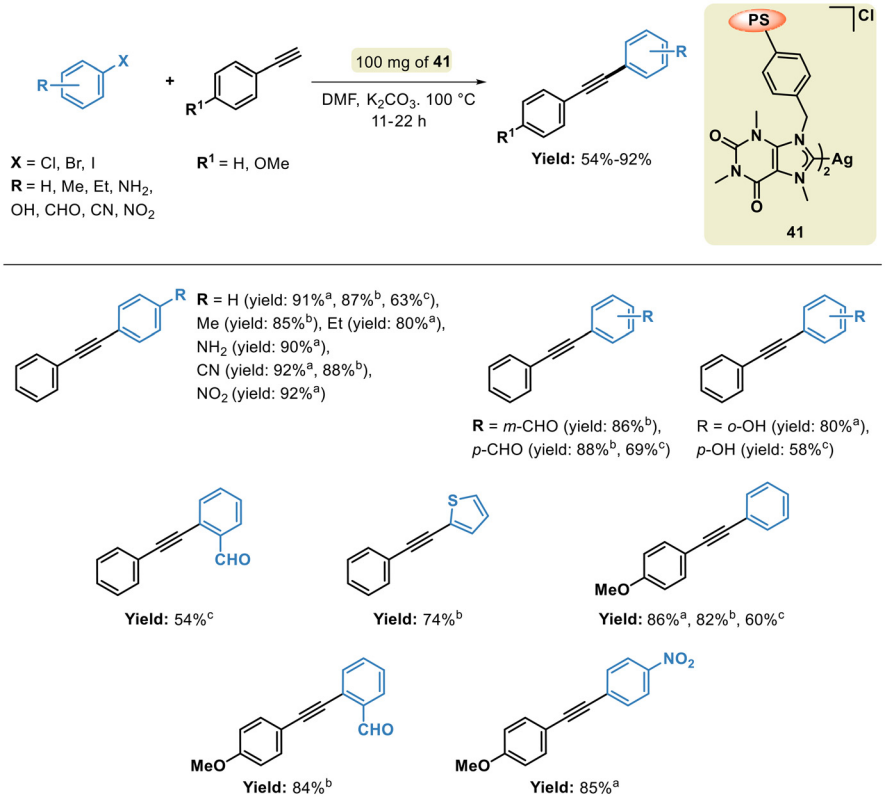

Scheme 26 Sonogashira reaction catalyzed by caffeine-based NHC complexes of Au. [a] Iodides. [b] Bromides. [c] Chlorides.

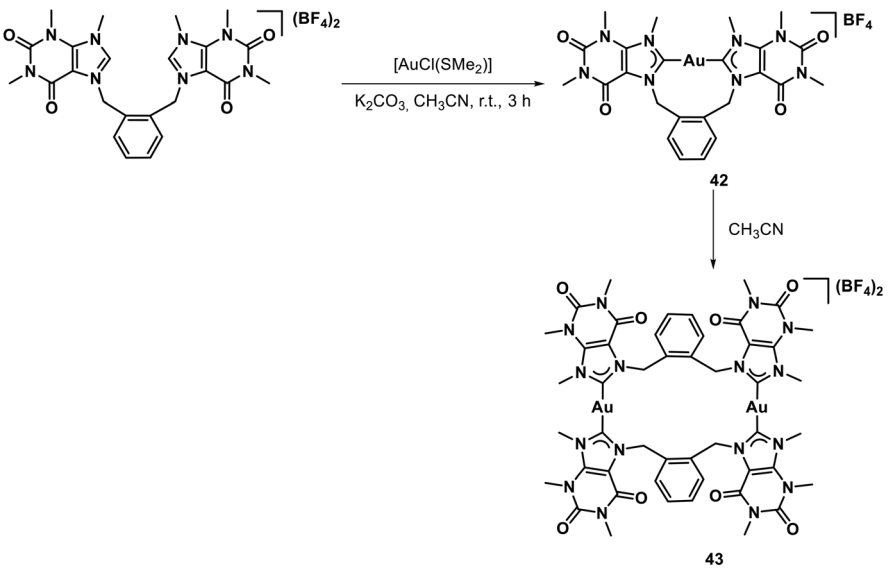

Scheme 27 Transformation of complex **42** into complex **43**.

process from silver (Scheme 28c). Interestingly, the presence of PF_6^- as the counterion in complex **45** leads to the formation of [$AgPF_6$], which can act as a halide scavenger in the presence of coordinating solvents. Complex **45** is air-stable up to its melting point. In the ^{13}C NMR spectrum, the carbene carbon resonates as a doublet at 188.46 ppm ($^1J_{C-Rh}$ = 43.8 Hz).[181]

Silver–NHC complexes readily undergo ligand transfer to palladium, providing a versatile and reliable route for the synthesis of NHC-Pd derivatives.

Scheme 29 summarizes several complexes obtained through this strategy.[182–184] The nature of the product depends strongly on the reaction conditions. When the reaction of [Ag

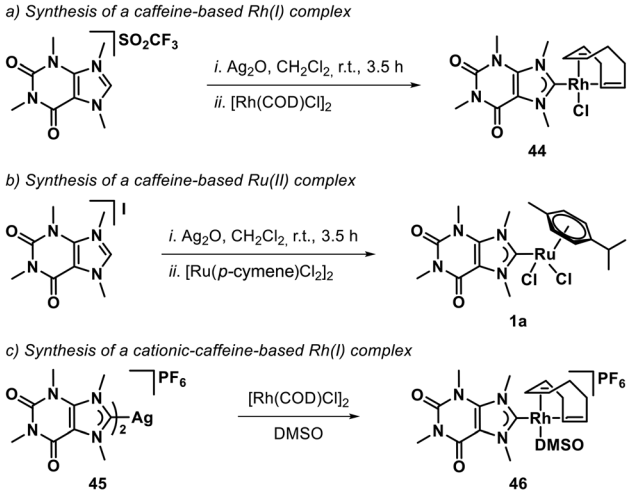

Scheme 28 Transmetalation from Ag(I)–NHC complexes to Ru(II) and Rh(I) centers.

(NHC)$_2$]X with a palladium precursor (*e.g.*, [PdCl(η^3-allyl)]$_2$, [(Me-Py-CH$_2$SPh)Pd(η^2-olefin)], or [PdC$_4$(COOMe)]$_n$) is performed in the presence of a neutral ligand (L)—such as phosphines or arsines—the resulting heteroleptic complex contains both the NHC and the neutral ligand. In contrast, under ligand-free conditions, bis(NHC)-Pd species are preferentially formed. The palladium complexes displayed significant cytotoxic activity toward selected cancer cell lines, suggesting potential for further bioorganometallic exploration.

For instance, the reaction of [Ag(NHC)$_2$]BF$_4$ with [PdCl(η^3-allyl)]$_2$ in the presence of two equivalents of triphenylphosphine afforded the heteroleptic complex (**47**). During this process, [AgBF$_4$] acts as a halide scavenger, removing the chloride ligand coordinated to palladium and generating a vacant coordination site that accommodates the phosphine ligand. Conversely, when the reaction is carried out in the absence of PPh$_3$, a cationic bis(NHC)–Pd complex (**48**) is obtained. The addition of KI effectively removes residual silver from the reac-

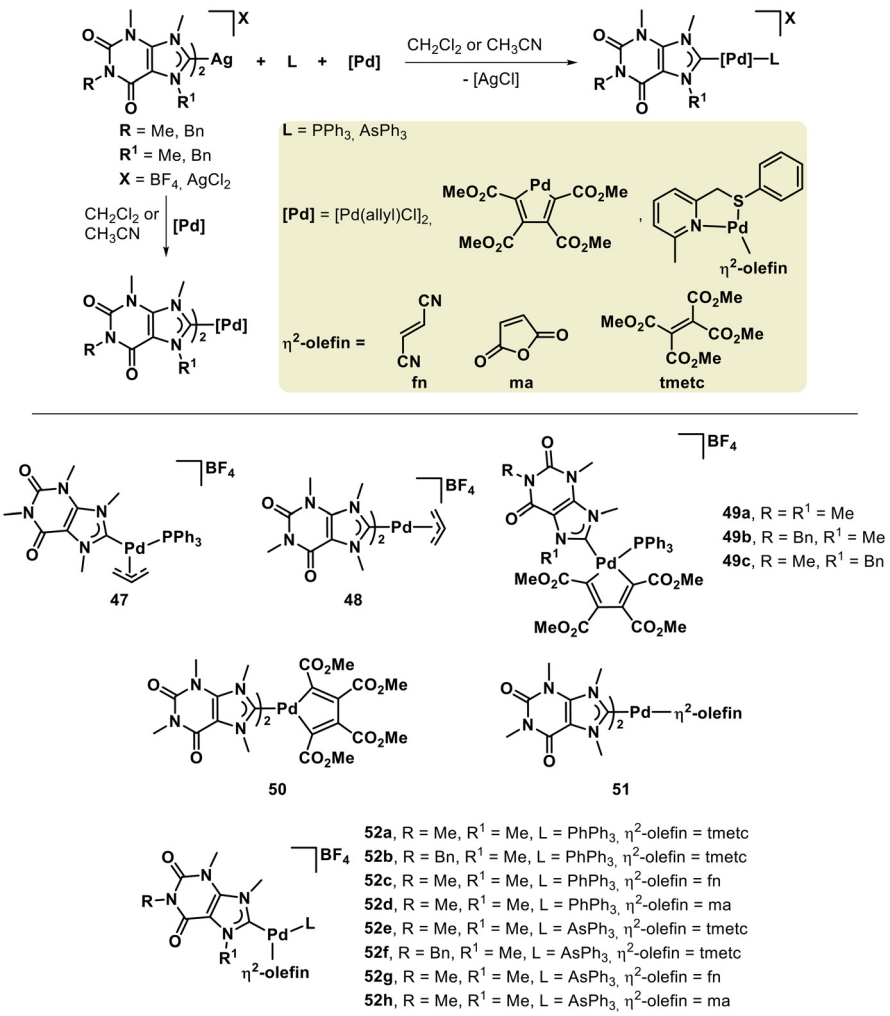

Scheme 29 Influence of neutral ligand addition on the formation of NHC-Pd(II) complexes, highlighting the generation of heteroleptic *versus* bis(NHC) species.

tion mixture, and the resulting cationic complexes are stable in air and in solution.

Similarly, cationic $[Ag(NHC)_2]AgCl_2$ reacts with equivalent amounts of the polymeric precursor $[PdC_4(COOMe)]_n$ in the presence of triphenylphosphine to afford heteroleptic complexes (**49a–c**) in up to 85% yield. In the absence of triphenylphosphine, bis(NHC)–Pd complexes are formed in moderate to good yields (71–90%), provided that thermodynamic and kinetic parameters are carefully controlled to prevent the formation of bis(PPh_3)-Pd or mixed-product distributions.

In a related approach, a library of NHC–Pd complexes (**52a–h**) was prepared by reacting equimolar amounts of $[Ag(NHC)_2]AgCl_2$ and PPh_3 (or $AsPh_3$) with [(Me-Py-CH_2SPh)Pd(η^2-olefin)] in CH_2Cl_2, where AgCl precipitation indicated reaction progress. This strategy takes advantage of the lability of the 2-methyl-6-((phenylthio)methyl)pyridine ligand, which is prone to dissociation due to chelate-ring distortion. The resulting heteroleptic complexes (**52a–h**) were isolated by ether precipitation or solvent evaporation, whereas bis(NHC)–Pd complexes (**51**) were obtained under ligand-free conditions.

Using $[Ag(NHC)_2]I$ (**53**) as a ligand-transfer reagent, the functionalized NHC–Pt complex (**55**)—bearing an all-nitrogen, methylated caffeine core ligand—was obtained indirectly *via* the intermediate formation of the NHC–Pt(dvtms) complex (**54**) (Scheme 30).[140] The reaction between complex **53** and $[Pt_2(dvtms)_3]$ first afforded complex **54**, which subsequently underwent oxidative addition of I_2 in the presence of the coordinating amine ligand $CyNH_2$, leading to complex **27** in 39% isolated yield on a gram scale (up to 2 g).

When complex **56** was dissolved in ethanol, methanol, or water/ethyl acetate mixtures and the solvent was allowed to slowly evaporate, the [Ag(NHC)OAc] complex (**57**) was obtained (Scheme 31).[185] Complex **57** is a water-soluble, light-stable solid, consistent with its formulation as an acetate derivative. Further ^{13}C NMR analysis showed a carbene carbon resonance at 186.2 ppm, along with carbonyl and methyl signals from the acetate group at 176.2 and 23.1 ppm, respectively, confirming the formation of the expected [Ag(NHC)OAc] complex (**57**).

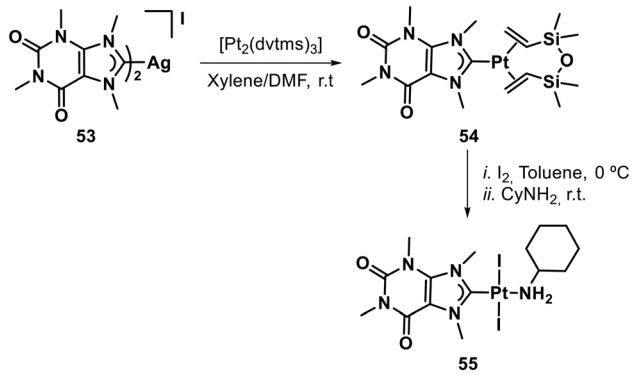

Scheme 30 Synthesis of Pt–NHC complexes *via* transmetalation from Ag(I)-NHC precursors.

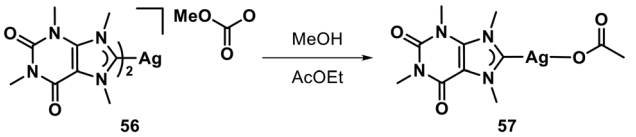

Scheme 31 Reaction of complex **56** leading to the formation of complex **57**.

6. Future outlook

Throughout this review, we have highlighted the growing importance of purine-derived NHC ligands as a versatile class of scaffolds for the stabilization of transition-metal centers and the promotion of a wide range of catalytic transformations. The complexes reported so far encompass Cu, Ni, Pd, Ag, Au, Rh, Ru, Ir, and Pt, representing nearly every major block of transition-metal catalysis. Collectively, these systems demonstrate how the unique structural and electronic characteristics of the purine nucleus—particularly its multiple heteroatom donors, accessible protonation sites, and distinct C–H activation potential—can be strategically harnessed to modulate metal–ligand bonding, reactivity, and selectivity.

From a synthetic perspective, the xanthine, theophylline, and caffeine backbones have proven to be the most accessible and tunable frameworks for generating purine-based NHCs. Their straightforward *N*-alkylation chemistry enables rapid post-functionalization to adjust steric and electronic properties, while the use of Ag-mediated transmetalation routes allows mild and selective access to a broad spectrum of M–NHC complexes without resorting to free carbene intermediates. Further advances in polymer- and graphene-supported systems highlight the compatibility of purine NHCs with heterogeneous catalysis, offering promising opportunities for catalyst recovery and recyclability, in line with green-chemistry principles.

Mechanistically, purine-derived NHC complexes reveal a striking range of behaviors across the periodic table. Group 8–10 metals (Fe, Ru, Os, Co, Rh, Ir, Ni, Pd, and Pt) typically engage in oxidative-addition/reductive-elimination cycles, benefitting from the strong σ-donor ability and tunable π-acceptor capacity of the purine carbene center. In particular, Ir(III) and Ru(II) complexes display rich C–H activation chemistry, accessible *mer*/*fac* isomerism, and notable photophysical properties, suggesting avenues toward photo-responsive or luminescent catalysts. In contrast, Group 11 metals (Cu, Ag, and Au) illustrate the complementary σ/π-activation and Lewis-acid pathways characteristic of late-d^{10} systems: Cu–NHC complexes excel in atom-economical C–N, C–O, and "click" transformations under mild conditions, whereas Ag– and Au–NHC complexes operate as soft Lewis acids in hydroamination and propargylamine synthesis, with Au uniquely capable of oxidative addition even in the absence of hemilabile co-ligands or external oxidants.

Looking ahead, the integration of purine-based NHCs into catalytic, photochemical, and biological contexts is poised to expand dramatically. The inherent biocompatibility and modular structure of purine ligands make them attractive not

only for homogeneous catalysis but also for bio-organometallic and medicinal applications, particularly when combined with Pt, Au, and Ru centers. Likewise, the development of Earth-abundant metal complexes (*e.g.*, Fe, Ni, Cu, and Co) featuring purine-derived NHCs will be central to advancing sustainable catalysis and C–H bond functionalization using renewable feedstocks.

In summary, purine-derived NHC ligands stand at the intersection of organic synthesis, coordination chemistry, and materials science, offering a rich platform for multifunctional catalyst design. Their electronic anisotropy, facile derivatization, and compatibility with diverse metals and supports ensure that future efforts will continue to uncover new reactivity paradigms, deepen our understanding of metal–carbene bonding, and foster environmentally responsible transformations driven by rational ligand design.

Author contributions

Conceptualization: D. M.-M., A. C.-R. and H. V.; writing – original draft preparation: A. C.-R. and H. V.; writing – review and editing: D. M.-M., A. C.-R., R. M.-C. and H. V.; visualization: D. M.-M., A. C.-R., R. M.-C. and H. V.; supervision: D. M.-M., A. C.-R. and H. V.; project administration: A. C.-R., H. V. and D. M.-M.; and funding acquisition: D. M.-M and H. V. All authors have read and agreed to the published version of the manuscript.

Conflicts of interest

The authors declare that they have no conflicts of interest.

Data availability

No primary research results, software or code have been included and no new data were generated or analysed as part of this review.

Acknowledgements

This research was supported by DGAPA-PAPIIT-UNAM and CONACYT. A. C.-R. thankfully acknowledges DGAPA/UNAM for a postdoctoral fellowship. R. M.-C. gratefully acknowledges the postgraduate fellowship provided by SECITHI with CVU 1079016. H. V. acknowledges financial support from the Universidad de Alcalá (PIUAH25/CC-074).

References

1 H. W. Wanzlick, *Angew. Chem., Int. Ed. Engl.*, 1962, **1**, 75–80.
2 H. W. Wanzlick and H. J. Schönherr, *Angew. Chem., Int. Ed. Engl.*, 1968, **7**, 141–142.
3 A. J. Arduengo III, R. L. Harlow and M. Kline, *J. Am. Chem. Soc.*, 1991, **113**, 361–363.
4 A. J. Arduengo III, M. Kline, J. C. Calabrese and F. Davidson, *J. Am. Chem. Soc.*, 1991, **113**, 9704–9705.
5 M. N. Hopkinson, C. Richter, M. Schedler and F. Glorius, *Nature*, 2014, **510**, 485–496.
6 E. Peris, *Chem. Rev.*, 2018, **118**, 9988–10031.
7 P. de Frémont, N. Marion and S. P. Nolan, *Coord. Chem. Rev.*, 2009, **253**, 862–892.
8 W. A. Herrmann, M. Elison, J. Fischer, C. Köcher and G. R. J. Artus, *Angew. Chem., Int. Ed. Engl.*, 1995, **34**, 2371–2374.
9 W. A. Herrmann, *Angew. Chem., Int. Ed.*, 2002, **41**, 1290–1309.
10 S. Budagumpi, R. S. Keri, G. Achar and K. N. Brinda, *Adv. Synth. Catal.*, 2020, **362**, 970–997.
11 A. Cervantes-Reyes, F. Rominger, M. Rudolph and A. S. K. Hashmi, *Adv. Synth. Catal.*, 2020, **362**, 2523–2533.
12 H. Clavier and S. P. Nolan, *Chem. Commun.*, 2010, **46**, 841–861.
13 A. Cervantes-Reyes, F. Rominger, M. Rudolph and A. S. K. Hashmi, *Chem. – Eur. J.*, 2019, **25**, 11745–11757.
14 E. L. Kolychev, A. F. Asachenko, P. B. Dzhevakov, A. A. Bush, V. V. Shuntikov, V. N. Khrustalev and M. S. Nechaev, *Dalton Trans.*, 2013, **42**, 6859–6866.
15 C. A. Urbina-Blanco, A. Leitgeb, C. Slugovc, X. Bantreil, H. Clavier, A. M. Z. Slawin and S. P. Nolan, *Chem. – Eur. J.*, 2011, **17**, 5045–5053.
16 A. Cervantes-Reyes, F. Rominger and A. S. K. Hashmi, *Chem. – Eur. J.*, 2020, **26**, 5530–5540.
17 H. V. Huynh, Y. Han, R. Jothibasu and J. A. Yang, *Organometallics*, 2009, **28**, 5395–5404.
18 D. J. Nelson and S. P. Nolan, *Chem. Soc. Rev.*, 2013, **42**, 6723–6753.
19 H. V. Huynh, *Chem. Rev.*, 2018, **118**, 9457–9492.
20 S. S. Bera, G. Utecht-Jarzyńska, S. Yang, S. P. Nolan and M. Szostak, *Chem. Rev.*, 2025, **125**, 5349–5435.
21 R. O. Pankov, D. O. Prima and V. P. Ananikov, *Coord. Chem. Rev.*, 2024, **516**, 215897.
22 A. Neshat, P. Mastrorilli and A. Mousavizadeh Mobarakeh, *Molecules*, 2022, **27**, 95.
23 C. Costabile, S. Pragliola and F. Grisi, *Symmetry*, 2022, **14**, 1615.
24 T. Zhou, G. Utecht-Jarzyńska and M. Szostak, *Coord. Chem. Rev.*, 2024, **512**, 215867.
25 A. Cervantes-Reyes, K. Farshadfar, M. Rudolph, F. Rominger, T. Schaub, A. Ariafard and A. S. K. Hashmi, *Green Chem.*, 2021, **23**, 889–897.
26 V. Dragutan, I. Dragutan, L. Delaude and A. Demonceau, *Coord. Chem. Rev.*, 2007, **251**, 765–794.
27 A. Kumari, *Sweet Biochemistry. Remembering Structures, Cycles, and Pathways by Mnemonics*, Academic Press, 2018.
28 M. Legraverend, *Tetrahedron*, 2008, **64**, 8585–8603.
29 T. Zhou, P. Gao, R. Lalancette, R. Szostak and M. Szostak, *Nat. Chem.*, 2024, **16**, 2025–2035.

30 L.Á Turcio-García, H. Valdés, S. Hernández-Ortega, D. Canseco-Gonzalez and D. Morales-Morales, *New J. Chem.*, 2022, **46**, 16789–16800.
31 L.Á Turcio-García, H. Valdés, A. Arenaza-Corona, S. Hernández-Ortega and D. Morales-Morales, *New J. Chem.*, 2023, **47**, 2090–2095.
32 L.Á Turcio-García, R. Parra-Unda, H. Valdés, S. Hernández-Ortega, G. G. Valenzuela-Ramirez, Y. P. Ahumada-Santos, Y. Sánchez-Lugo, V. Reyes-Márquez and D. Morales-Morales, in *Pharmaceutics*, 2025, pp. 973.
33 S. C. Scott, J. A. Cadge, G. K. Boden, J. F. Bower and C. A. Russell, *Angew. Chem., Int. Ed.*, 2023, **62**, e202301526.
34 P. Gao, J. Xu, T. Zhou, Y. Liu, E. Bisz, B. Dziuk, R. Lalancette, R. Szostak, D. Zhang and M. Szostak, *Angew. Chem., Int. Ed.*, 2023, **62**, e202218427.
35 G. Galdi and C. Costabile, *Chem. – Eur. J.*, 2024, **30**, e202402774.
36 M. Alcarazo, T. Stork, A. Anoop, W. Thiel and A. Fürstner, *Angew. Chem., Int. Ed.*, 2010, **49**, 2542–2546.
37 T. Scattolin, G. Andreetta, M. Mauceri, F. Rizzolio, N. Demitri, V. Canzonieri and F. Visentin, *J. Organomet. Chem.*, 2021, **952**, 122014.
38 C. Stoll, C. Besnard and C. Mazet, *JACS Au*, 2025, **5**, 4681–4687.
39 T. Zhou, C. Zhao, S. Yang, E. Bisz, B. Dziuk, R. Lalancette, R. Szostak, X. Hong and M. Szostak, *ACS Catal.*, 2025, **15**, 13846–13859.
40 T. Sheikh Mohammad, P. Sakharov, S. Raje and G. de Ruiter, *ACS Catal.*, 2025, **15**, 5370–5377.
41 T. S. Mohammad, Y. Jin, S. Raje, K. Młodzikowska-Pieńko, Z.-X. Yu and G. de Ruiter, *J. Am. Chem. Soc.*, 2025, **147**, 15195–15204.
42 K. Azouzi, R. Pointis, R. Buhaibeh, P. H. Fernández, L. Pedussaut, M. Boundor, A. Bonfiglio, A. Bruneau-Voisine, D. Wei, T. Roisnel, C. Duhayon, M.Á Casado, D. A. Valyaev, Y. Canac, S. Bastin, C. Raynaud and J.-B. Sortais, *J. Catal.*, 2024, **430**, 115334.
43 J.-P. Chang, Y.-W. Zhang, L.-Y. Sun, L. Zhang, F. E. Hahn and Y.-F. Han, *Angew. Chem., Int. Ed.*, 2024, **63**, e202409664.
44 Y.-W. Zhang, Y. Lu, L.-Y. Sun, P. D. Dutschke, M.-M. Gan, L. Zhang, A. Hepp, Y.-F. Han and F. E. Hahn, *Angew. Chem., Int. Ed.*, 2023, **62**, e202312323.
45 R. Kumar, M. K. Pandey, A. Bhandari and J. Choudhury, *ACS Catal.*, 2023, **13**, 4824–4834.
46 V. K. Rawat, K. Higashida and M. Sawamura, *ACS Catal.*, 2022, **12**, 8325–8330.
47 S. Tang, Y. Zhao and K. Nozaki, *J. Am. Chem. Soc.*, 2021, **143**, 17953–17957.
48 S. Garhwal, A. Kaushansky, N. Fridman and G. de Ruiter, *Chem Catal.*, 2021, **1**, 631–647.
49 S. Garhwal, A. Kaushansky, N. Fridman, L. J. W. Shimon and G. d. Ruiter, *J. Am. Chem. Soc.*, 2020, **142**, 17131–17139.
50 S. Byun, S. Park, Y. Choi, J. Y. Ryu, J. Lee, J.-H. Choi and S. Hong, *ACS Catal.*, 2020, **10**, 10592–10601.
51 Y.-W. Zhang, S. Bai, Y.-Y. Wang and Y.-F. Han, *J. Am. Chem. Soc.*, 2020, **142**, 13614–13621.
52 L. Li, F. Han, X. Nie, Y. Hong, S. Ivlev and E. Meggers, *Angew. Chem., Int. Ed.*, 2020, **59**, 12392–12395.
53 D.-A. Park, S. Byun, J. Y. Ryu, J. Lee, J. Lee and S. Hong, *ACS Catal.*, 2020, **10**, 5443–5453.
54 Y. Tang, I. Benaissa, M. Huynh, L. Vendier, N. Lugan, S. Bastin, P. Belmont, V. César and V. Michelet, *Angew. Chem., Int. Ed.*, 2019, **58**, 7977–7981.
55 C. B. Schwamb, K. P. Fitzpatrick, A. C. Brueckner, H. C. Richardson, P. H. Y. Cheong and K. A. Scheidt, *J. Am. Chem. Soc.*, 2018, **140**, 10644–10648.
56 H. Yasuda, R. Nakano, S. Ito and K. Nozaki, *J. Am. Chem. Soc.*, 2018, **140**, 1876–1883.
57 R. Nakano and K. Nozaki, *J. Am. Chem. Soc.*, 2015, **137**, 10934–10937.
58 C. T. Check, K. P. Jang, C. B. Schwamb, A. S. Wong, M. H. Wang and K. A. Scheidt, *Angew. Chem., Int. Ed.*, 2015, **54**, 4264–4268.
59 A. Schmidt, N. Grover, T. K. Zimmermann, L. Graser, M. Cokoja, A. Pöthig and F. E. Kühn, *J. Catal.*, 2014, **319**, 119–126.
60 M. Alcarazo, S. J. Roseblade, A. R. Cowley, R. Fernández, J. M. Brown and J. M. Lassaletta, *J. Am. Chem. Soc.*, 2005, **127**, 3290–3291.
61 H. Ashihara, K. Mizuno, T. Yokota and A. Crozier, Xanthine Alkaloids: Occurrence, Biosynthesis, and Function in Plants, in *Progress in the Chemistry of Organic Natural Products 105*, ed. A. D. Kinghorn, H. Falk, S. Gibbons and J. i. Kobayashi, Springer International Publishing, Cham, 2017, pp. 1–88.
62 A. Chaudhary, D. Mathur, R. Gaba, R. Pasricha and K. Sharma, *RSC Adv.*, 2024, **14**, 8932–8962.
63 F. P. L. Lim and A. V. Dolzhenko, *Eur. J. Med. Chem.*, 2014, **85**, 371–390.
64 A. Szadkowska, S. Staszko, E. Zaorska and R. Pawłowski, *RSC Adv.*, 2016, **6**, 44248–44253.
65 N. U. D. Reshi and J. K. Bera, *Coord. Chem. Rev.*, 2020, **422**, 213334.
66 A. Sánchez-Mora, L. González-Sebastián, J. A. Cruz-Navarro, A. Arenaza-Corona, T. Ramírez-Apan, A. Nieto-Camacho and D. Morales-Morales, *New J. Chem.*, 2025, **49**, 18258–18269.
67 M. O. Dar, R. H. Mir, R. Mohiuddin, M. H. Masoodi and F. A. Sofi, *J. Inorg. Biochem.*, 2023, **246**, 112290.
68 G. Francescato, M. I. P. S. Leitão, G. Orsini and A. Petronilho, *ChemMedChem*, 2024, **19**, e202400118.
69 H. Valdés, D. Canseco-González, J. M. Germán-Acacio and D. Morales-Morales, *J. Organomet. Chem.*, 2018, **867**, 51–54.
70 S. A. J. Almahmoud, M. Cariello and A. O. Elzupir, *Orient. J. Chem.*, 2023, **39**, 222–230.
71 H. Song and H.-B. Kraatz, *Inorg. Chim. Acta*, 2009, **362**, 1365–1368.
72 M. Campitiello, A. Cremonini, M. A. Squillaci, S. Pieraccini, A. Ciesielski, P. Samorì and S. Masiero, *J. Org. Chem.*, 2021, **86**, 9970–9978.

73 N. J. Forrow, N. C. Foulds, J. E. Frew and J. T. Law, *Bioconjugate Chem.*, 2004, **15**, 137–144.
74 C. M. Mikulski, M. L. Bayne, S. Grossman, M. Gaul, A. Renn, D. L. Staley and N. M. Karayannis, *J. Coord. Chem.*, 1989, **20**, 185–191.
75 C. M. Mikulski, S. Grossman, M. L. Bayne, M. Gaul, D. Kanach, K. Udell and N. M. Karayannis, *J. Coord. Chem.*, 1990, **22**, 175–182.
76 C. M. Mikulski, S. Grossman, M. L. Bayne, M. Gaul, D. Kanach, K. Udell and N. M. Karayannis, *Inorg. Chim. Acta*, 1990, **173**, 31–35.
77 M. M. Alam, M. J. Mia, M. A. A. Mamun, S. S. Rakhi, K. A. Azam and S. Ghosh, *J. Organomet. Chem.*, 2021, **944**, 121791.
78 K. Sayin and A. Üngördü, *Spectrochim. Acta, Part A*, 2018, **193**, 147–155.
79 F. Mazars and L. Delaude, *Organometallics*, 2023, **42**, 1589–1597.
80 J. Canivet and G. Süss-Fink, *Green Chem.*, 2007, **9**, 391–397.
81 J. Gunasekaran, S. Muthuselvan, D. Annadurai, D. B. Christopher Leslee, N. Venkatesan, S. Murthy, B. Ramasamy, L. G. Alves, A. M. Martins and S. B. Kuppannan, *J. Mol. Struct.*, 2024, **1309**, 138179.
82 F. Pirani and H. Eshghi, *Inorg. Chem. Commun.*, 2025, **181**, 115297.
83 J. Liquier-Milward, *Nature*, 1951, **167**, 1068–1069.
84 A. Singh, S. K. Maiti, H. P. Gogoi and P. Barman, *Polyhedron*, 2023, **230**, 116244.
85 S. D. K. Alzamili, *Res. J. Chem. Environ.*, 2022, **26**, 129–141.
86 H.-K. Zhao, H.-W. Yang, X.-G. Wang, B. Ding, Z.-Y. Liu, X.-J. Zhao and E.-C. Yang, *Inorg. Chem. Commun.*, 2019, **107**, 107483.
87 H. E. Hamdani, M. E. Amane and C. Duhayon, *J. Mol. Struct.*, 2019, **1190**, 125–134.
88 H. E. Hamdani and M. E. Amane, *J. Mol. Struct.*, 2019, **1184**, 262–270.
89 Ö. Altun and M. Şuözer, *J. Mol. Struct.*, 2017, **1149**, 307–314.
90 S. S. Bera and M. Szostak, *ACS Catal.*, 2022, **12**, 3111–3137.
91 I. Eslava-Gonzalez, H. Valdés, M. Teresa Ramírez-Apan, S. Hernandez-Ortega, M. Rosario Zermeño-Ortega, A. Avila-Sorrosa and D. Morales-Morales, *Inorg. Chim. Acta*, 2020, **507**, 119588.
92 Q. Zhao, G. Meng, S. P. Nolan and M. Szostak, *Chem. Rev.*, 2020, **120**, 1981–2048.
93 H. Buhl and C. Ganter, *J. Organomet. Chem.*, 2016, **809**, 74–78.
94 P. V. Simpson, K. Radacki, H. Braunschweig and U. Schatzschneider, *J. Organomet. Chem.*, 2015, **782**, 116–123.
95 D. G. Gusev and E. Peris, *Dalton Trans.*, 2013, **42**, 7359–7364.
96 A. R. Chianese, X. Li, M. C. Janzen, J. W. Faller and R. H. Crabtree, *Organometallics*, 2003, **22**, 1663–1667.
97 R. A. Kelly III, H. Clavier, S. Giudice, N. M. Scott, E. D. Stevens, J. Bordner, I. Samardjiev, C. D. Hoff, L. Cavallo and S. P. Nolan, *Organometallics*, 2008, **27**, 202–210.
98 B. Joshi and M. Shivashankar, *ACS Omega*, 2023, **8**, 43408–43432.
99 A. Sebris, M. Guzauskas, M. Mahmoudi, D. Volyniuk, J. V. Grazulevicius, A. Mishnev, I. Novosjolova, M. Turks, G. Jonusauskas and K. Traskovskis, *J. Mater. Chem. C*, 2023, **11**, 14608–14620.
100 M. Bevilacqua, V. Giuso, M. Rancan, L. Armelao, C. Graiff, W. Baratta, V. Di Marco and A. Biffis, *Eur. J. Inorg. Chem.*, 2022, **2022**, e202200484.
101 R. N. Osorio Yáñez, A. Hepp, T. T. Y. Tan and F. E. Hahn, *Organometallics*, 2020, **39**, 344–352.
102 D. Brackemeyer, C. Schulte to Brinke, F. Roelfes and F. E. Hahn, *Dalton Trans.*, 2017, **46**, 4510–4513.
103 S. Kuwata and F. E. Hahn, *Chem. Rev.*, 2018, **118**, 9642–9677.
104 S. Cepa, C. Schulte to Brinke, F. Roelfes and F. E. Hahn, *Organometallics*, 2015, **34**, 5454–5460.
105 D. Brackemeyer, A. Hervé, C. Schulte to Brinke, M. C. Jahnke and F. E. Hahn, *J. Am. Chem. Soc.*, 2014, **136**, 7841–7844.
106 A. Makhloufi, W. Frank and C. Ganter, *Organometallics*, 2012, **31**, 7272–7277.
107 J. Schütz and W. A. Herrmann, *J. Organomet. Chem.*, 2004, **689**, 2995–2999.
108 S. C. Zinner, C. F. Rentzsch, E. Herdtweck, W. A. Herrmann and F. E. Kühn, *Dalton Trans.*, 2009, 7055–7062.
109 C. F. Rentzsch, E. Tosh, W. A. Herrmann and F. E. Kühn, *Green Chem.*, 2009, **11**, 1610–1617.
110 M. Bortenschlager, J. Schütz, D. von Preysing, O. Nuyken, W. A. Herrmann and R. Weberskirch, *J. Organomet. Chem.*, 2005, **690**, 6233–6237.
111 E. A. B. Kantchev, C. J. O'Brien and M. G. Organ, *Angew. Chem., Int. Ed.*, 2007, **46**, 2768–2813.
112 A. Kumar, M. Kumar and A. K. Verma, *J. Org. Chem.*, 2020, **85**, 13983–13996.
113 S. B. Umabharathi, M. Neetha and G. Anilkumar, *Top. Curr. Chem.*, 2024, **382**, 3.
114 P. Ruiz-Castillo and S. L. Buchwald, *Chem. Rev.*, 2016, **116**, 12564–12649.
115 N. Selander and K. J. Szabó, *Chem. Rev.*, 2011, **111**, 2048–2076.
116 F.-S. Han, *Chem. Soc. Rev.*, 2013, **42**, 5270–5298.
117 B. M. Rosen, K. W. Quasdorf, D. A. Wilson, N. Zhang, A.-M. Resmerita, N. K. Garg and V. Percec, *Chem. Rev.*, 2011, **111**, 1346–1416.
118 A. A. Danopoulos, T. Simler and P. Braunstein, *Chem. Rev.*, 2019, **119**, 3730–3961.
119 E. Rufino-Felipe, H. Valdés and D. Morales-Morales, *Eur. J. Org. Chem.*, 2022, e202200654.
120 E. Marín-Carrillo, H. Valdés, S. Hernández-Ortega and D. Morales-Morales, *Inorg. Chim. Acta*, 2023, **548**, 121365.

121 S. Díez-González, N. Marion and S. P. Nolan, *Chem. Rev.*, 2009, **109**, 3612–3676.
122 V. V. Sharutin and A. R. Zykova, *Rev. Adv. Chem.*, 2023, **13**, 111–151.
123 A. Jayaraj, A. V. Raveedran, A. T. Latha, D. Priyadarshini and P. C. A. Swamy, *Coord. Chem. Rev.*, 2023, **478**, 214922.
124 S. Zhao, Z. Yang, G. Jiang, S. Huang, M. Bian, Y. Lu and W. Liu, *Coord. Chem. Rev.*, 2021, **449**, 214217.
125 J. Zhang, M. M. Rahman, Q. Zhao, J. Feliciano, E. Bisz, B. Dziuk, R. Lalancette, R. Szostak and M. Szostak, *Organometallics*, 2022, **41**, 1806–1815.
126 H. A. Mohamed, B. R. M. Lake, T. Laing, R. M. Phillips and C. E. Willans, *Dalton Trans.*, 2015, **44**, 7563–7569.
127 A. Gómez-Suárez, D. J. Nelson and S. P. Nolan, *Chem. Commun.*, 2017, **53**, 2650–2660.
128 T. Aalhusaini, D. Pore and G. Rashinkar, *J. Organomet. Chem.*, 2025, **1034**, 123637.
129 https://www.nobelprize.org/prizes/chemistry/2010/summary/.
130 F.-T. Luo and H.-K. Lo, *J. Organomet. Chem.*, 2011, **696**, 1262–1265.
131 T. Scattolin, L. Canovese, F. Visentin, S. Paganelli, P. Canton and N. Demitri, *Appl. Organomet. Chem.*, 2018, **32**, e4034.
132 F. Mazars, G. Zaragoza and L. Delaude, *J. Organomet. Chem.*, 2022, **978**, 122489.
133 M. M. Rahman, J. Zhang, Q. Zhao, J. Feliciano, E. Bisz, B. Dziuk, R. Lalancette, R. Szostak and M. Szostak, *Organometallics*, 2022, **41**, 2281–2290.
134 E. Mohammadi and B. Movassagh, *J. Organomet. Chem.*, 2016, **822**, 62–66.
135 O. Bysewski, A. Winter and U. S. Schubert, *Inorganics*, 2023, **11**, 164.
136 S. Khot, P. Dandge, S. Shikalgar, P. Ghule, D. Pore and G. Rashinkar, *J. Organomet. Chem.*, 2025, **1041**, 123831.
137 F. Mazars, K. S. Etsè, G. Zaragoza and L. Delaude, *J. Organomet. Chem.*, 2024, **1003**, 122928.
138 Q. Teng, Y. Zhao, Y. Lu, Z. Liu, H. Chen, D. Yuan, H. V. Huynh and Q. Meng, *Organometallics*, 2022, **41**, 161–168.
139 V. R. Landaeta, R. E. Rodríguez-Lugo, E. N. Rodríguez-Arias, D. S. Coll-Gómez and T. González, *Transition Met. Chem.*, 2010, **35**, 165–175.
140 M. Skander, P. Retailleau, B. Bourrié, L. Schio, P. Mailliet and A. Marinetti, *J. Med. Chem.*, 2010, **53**, 2146–2154.
141 J. J. Hu, S.-Q. Bai, H. H. Yeh, D. J. Young, Y. Chi and T. S. A. Hor, *Dalton Trans.*, 2011, **40**, 4402–4406.
142 J.-J. Zhang, C.-M. Che and I. Ott, *J. Organomet. Chem.*, 2015, **782**, 37–41.
143 O. S. Wenger, *J. Am. Chem. Soc.*, 2018, **140**, 13522–13533.
144 F. Lazreg, F. Nahra and C. S. J. Cazin, *Coord. Chem. Rev.*, 2015, **293–294**, 48–79.
145 W.-J. Yoo, T. V. Q. Nguyen and S. Kobayashi, *Angew. Chem., Int. Ed.*, 2014, **53**, 10213–10217.
146 M. R. Uehling, A. M. Suess and G. Lalic, *J. Am. Chem. Soc.*, 2015, **137**, 1424–1427.
147 F. Sebest, J. J. Dunsford, M. Adams, J. Pivot, P. D. Newman and S. Díez-González, *ChemCatChem*, 2018, **10**, 2041–2045.
148 N. K. Devaraj and M. G. Finn, *Chem. Rev.*, 2021, **121**, 6697–6698.
149 M. Meldal and C. W. Tornøe, *Chem. Rev.*, 2008, **108**, 2952–3015.
150 Widespread applications of copper-catalyzed click reactions guided profound advances in organic chemistry, drug discovery, biomaterials and agrochemical synthesis, among other research fields, which honored pioneering efforts of Carolyn R. Bertozzi, P. Morten, and K. B. Sharpless awarded with the 2022 Nobel Prize in Chemistry, see: https://www.nobelprize.org/prizes/chemistry/2022/summary/.
151 R. Dorel and A. M. Echavarren, *Chem. Rev.*, 2015, **115**, 9028–9072.
152 A. S. K. Hashmi, *Chem. Rev.*, 2007, **107**, 3180–3211.
153 R. P. Herrera and M. C. Gimeno, *Chem. Rev.*, 2021, **121**, 8311–8363.
154 E. Jiménez-Núñez and A. M. Echavarren, *Chem. Rev.*, 2008, **108**, 3326–3350.
155 Z. Li, C. Brouwer and C. He, *Chem. Rev.*, 2008, **108**, 3239–3265.
156 C. Nevado, *Chimia*, 2010, **64**, 247–251.
157 T. N. Aalhusaini, W. N. Al-darkazali, D. Pore and G. Rashinkar, *J. Organomet. Chem.*, 2025, **1039**, 123752.
158 A. Mariconda, D. Iacopetta, M. Sirignano, J. Ceramella, A. D'Amato, M. Marra, M. Pellegrino, M. S. Sinicropi, S. Aquaro and P. Longo, *Int. J. Mol. Sci.*, 2024, **25**, 2599.
159 T. Aalhusaini, D. Pore and G. Rashinkar, *J. Organomet. Chem.*, 2025, **1023**, 123406.
160 M. Font, F. Acuña-Parés, T. Parella, J. Serra, J. M. Luis, J. Lloret-Fillol, M. Costas and X. Ribas, *Nat. Commun.*, 2014, **5**, 4373.
161 L. Demonti, D. Joven-Sancho, M. Baya and N. Nebra, *Chem. – Eur. J.*, 2025, **31**, e202501606.
162 E. M. H. Larsen, T. Brock-Nannestad, J. Skibsted, A. Reinholdt and J. Bendix, *Chem. Sci.*, 2024, **15**, 18067–18075.
163 L. Demonti, D. Joven-Sancho, N. Saffon-Merceron, M. Baya and N. Nebra, *Chem. – Eur. J.*, 2024, **30**, e202400881.
164 L. Demonti, D. Joven-Sancho and N. Nebra, *Chem. Rec.*, 2023, **23**, e202300143.
165 L. Demonti, H. Tabikh, N. Saffon-Merceron and N. Nebra, *Eur. J. Inorg. Chem.*, 2023, **26**, e202300042.
166 C. M. Lemon, D. C. Powers, M. Huynh, A. G. Maher, A. A. Phillips, B. P. Tripet and D. G. Nocera, *Inorg. Chem.*, 2023, **62**, 3–17.
167 L. Demonti, N. Saffon-Merceron, N. Mézailles and N. Nebra, *Chem. – Eur. J.*, 2021, **27**, 15396–15405.
168 D. Joven-Sancho, M. Baya, L. R. Falvello, A. Martín, J. Orduna and B. Menjón, *Chem. – Eur. J.*, 2021, **27**, 12796–12806.
169 M. Deuker, Y. Yang, R. A. J. O'Hair and K. Koszinowski, *Organometallics*, 2021, **40**, 2354–2363.
170 X. Ribas, L. Capdevila and P. Font, 6.13 - High-Valent Cu, Ag, and Au Coordination Compounds, in *Comprehensive*

Coordination Chemistry III, ed. E. C. Constable, G. Parkin and L. Que Jr., Elsevier, Oxford, 2021, pp. 474–516.

171 D. Joven-Sancho, M. Baya, A. Martín, J. Orduna and B. Menjón, *Chem. – Eur. J.*, 2020, **26**, 4471–4475.

172 L. Capdevila, E. Andris, A. Briš, M. Tarrés, S. Roldán-Gómez, J. Roithová and X. Ribas, *ACS Catal.*, 2018, **8**, 10430–10436.

173 S. Weske, R. A. Hardin, T. Auth, R. A. J. O'Hair, K. Koszinowski and C. A. Ogle, *Chem. Commun.*, 2018, **54**, 5086–5089.

174 M. Font and X. Ribas, Pincerlike Cyclic Systems for Unraveling Fundamental Coinage Metal Redox Processes, in *The Privileged Pincer-Metal Platform: Coordination Chemistry & Applications*, ed. G. van Koten and R. A. Gossage, Springer International Publishing, Cham, 2016, pp. 269–306.

175 V. Stoppa, T. Scattolin, M. Bevilacqua, M. Baron, C. Graiff, L. Orian, A. Biffis, I. Menegazzo, M. Roverso, S. Bogialli, F. Visentin and C. Tubaro, *New J. Chem.*, 2021, **45**, 961–971.

176 A. Cervantes-Reyes, T. Saxl, P. M. Stein, M. Rudolph, F. Rominger, A. M. Asiri and A. S. K. Hashmi, *ChemSusChem*, 2021, **14**, 2367–2374.

177 G. Fang and X. Bi, Silver Complexes in Organic Transformations, in *Silver Catalysis in Organic Synthesis*, 2019, pp. 661–722.

178 K. Yamashita, S. Hase, Y. Kayaki and T. Ikariya, *Org. Lett.*, 2015, **17**, 2334–2337.

179 Y. Li, X. Chen, Y. Song, L. Fang and G. Zou, *Dalton Trans.*, 2011, **40**, 2046–2052.

180 J.-J. Zhang, J. K. Muenzner, M. A. Abu el Maaty, B. Karge, R. Schobert, S. Wölfl and I. Ott, *Dalton Trans.*, 2016, **45**, 13161–13168.

181 A. Kascatan-Nebioglu, M. J. Panzner, J. C. Garrison, C. A. Tessier and W. J. Youngs, *Organometallics*, 2004, **23**, 1928–1931.

182 T. Scattolin, N. Pangerc, I. Lampronti, C. Tupini, R. Gambari, L. Marvelli, F. Rizzolio, N. Demitri, L. Canovese and F. Visentin, *J. Organomet. Chem.*, 2019, **899**, 120857.

183 T. Scattolin, S. Giust, P. Bergamini, I. Caligiuri, L. Canovese, N. Demitri, R. Gambari, I. Lampronti, F. Rizzolio and F. Visentin, *Appl. Organomet. Chem.*, 2019, **33**, e4902.

184 T. Scattolin, I. Caligiuri, L. Canovese, N. Demitri, R. Gambari, I. Lampronti, F. Rizzolio, C. Santo and F. Visentin, *Dalton Trans.*, 2018, **47**, 13616–13630.

185 A. Kascatan-Nebioglu, A. Melaiye, K. Hindi, S. Durmus, M. J. Panzner, L. A. Hogue, R. J. Mallett, C. E. Hovis, M. Coughenour, S. D. Crosby, A. Milsted, D. L. Ely, C. A. Tessier, C. L. Cannon and W. J. Youngs, *J. Med. Chem.*, 2006, **49**, 6811–6818.